1 HEAT REMOVAL FROM NUCLEAR REACTORS

In this chapter, we will discuss the thermal design of nuclear reactors. During this discussion the concepts introduced in the previous chapters will be widely used.

In nuclear reactors, the fission is the origin of the thermal energy generation. In heterogeneous reactors, the thermal energy released by fission in the fuel rods is transferred by heat conduction to the surface of the rod and then by convection to the coolant which circulates around the rods. The coolants transports the thermal energy released by fission in the reactor to external heat exchangers called steam generators in which a high quality steam is generated for use in the steam cycle associated with the nuclear reactor. A good efficiency of this steam cycle requires a high coolant temperature. However, a high coolant temperature causes high temperature in the fuel rods. Because of the metallurgical limitations it is impossible to push the fuel and cladding temperature beyond certain limit. These temperatures also set a limit to the fission power that can be released within the fuel rods, i.e., within the reactor core.

The circulation of the coolant in the reactor core is assured by a pump. For a good efficiency of the power plant, we should extract maximum thermal energy with minimum pumping power. It is well known fact that there is no theoretical upper limit to the rate of energy release, i.e., of power production, due to fission. The question is that how this energy can be removed while maintaining the temperatures throughout the reactor core at reasonable levels. At the first glance, we may think that for a given reactor, we may remove more and more energy by increasing the coolant flow rate. This can be achieved by increasing the velocity of the coolant or the flow section of the coolant through the fuel channel. Obviously, the latter solution is not very desirable because its negative effect on the multiplication factor. We know that an increase in coolant flow rate will require higher pumping power. Consequently, it is important to verify how far the coolant flow rate could be pushed while ensuring a maximum mechanical energy output from the power plant and in the same time avoiding any nuclear core design problems, keeping the temperatures at acceptable levels and also avoiding mechanical problems such as vibrations and thermal stresses. It is also possible to increase the removed energy by:

1. replacing the coolant by an other with better thermal properties, i.e., replace a gas coolant (CO_2 , for example) with a liquid coolant (light or heavy water),
2. increasing the contact area between the coolant and the fuel rod; this can be achieved by adding auxiliary heat transfer surfaces to the fuel rod (fins) or by subdividing a big diameter rod into smaller diameter rods, or
3. by using the boiling phenomenon.

However, before proceeding with the above solutions, their impact on the nuclear design of the reactor core should be thoroughly checked. We should keep in mind that a compromise is always necessary between the nuclear and thermal design of a reactor.

In this chapter, we will mainly study the temperature distribution in a reactor core. We will consider the type of reactor in which the fuel rods (or fuel bundles) are placed in channels which run

through the reactor core. The coolant circulates around the rods. The shape of the core is cylindrical in form and surrounded by lateral and axial reflectors or only by a lateral reflector as in the CANDU reactors. As we know, the reflectors cause some of the leaking neutrons to return to the reactor core.

1.1 Generation of Heat in Nuclear Reactors

1.1.1 Thermal Energy Release During Fission

The thermal energy released in nuclear reactors is due to the fission process and at a much smaller degree to the non-fission neutron capture in the fuel, moderator, coolant and structural material. Approximately 207 Mev of energy is emitted during a fission and the distribution of this energy among different components of a neutron-induced fission of ^{235}U is given in Table 7.1.

Table 7.1 Emitted and recoverable energies for fission of ^{235}U

Components	Emitted energy	Energy converted to heat or recovered energy	
	Mev	Mev	% of total
Fission fragments	168	168	84
Neutrons	5	5	2.5
Prompt γ rays	7	7	3.5
Delayed radiations:			
β–rays	8	8	4
γ-rays	7	7	3.5
neutrinos	12	-	-
Capture γ-rays	-	5	2.5
TOTAL	207	200	100

Table 7.1 also includes the energy converted into heat or the recoverable energy. We observe that the emitted energy and the recoverable energy are different. This is due to the fact that in the energy emitted during the fission process, the kinetic energy of the fission fragments, neutrons, gammas and betas are converted into heat in the reactor core and shielding material whereas the neutrinos which accompany β-decay escape from the reactor virtually without any interaction, i.e., any energy deposit. Therefore in the column of "energy converted to heat," neutrinos are ignored. Furthermore, in the same column a new item which consists of "capture γ-rays" has been included. The capture γ-rays or radiative capture reactions account for (ν-1) neutrons per fission (ν is the average number of neutrons emitted per fission; ν is approximately equal to 2.5 for ^{235}U) which are absorbed parasitically in the reactor without producing any fission reaction. Each absorption results with the production of one or more capture γ-rays, whose energies depend on the binding energy of the neutrons to the compound nucleus. Consequently, the contribution of the radiative capture to the energy converted to heat depends on the composition of materials (fissile, fertile, coolant, moderator and structure) which constitute the reactor. From about 3 to 12 Mev of

capture γ-radiation is produced per fission; an average value of 5 Mev is included in Table 7.1. All this γ-ray, as already pointed out, is recoverable for the reactor system.

As indicated in Table 7.1, almost 84% and 4% of the energy converted to heat are due to the fission fragments and to the β-rays, respectively. The very short range of fission fragments (10^{-2} mm from the fission site) and β-rays (<1 mm) ensures that this heat release takes place within the fuel elements. The energy release during neutron thermalization takes place in the moderator. The energy release due to neutron capture occurs largely within the fuel; a small portion of this energy is released in the structural material, in the moderator and in the coolant. The gamma rays have longer ranges. Because of the large mass of the fuel and its heavy density, substantial portion of the γ-rays is absorbed in the fuel and the rest in the moderator and the structural material. In large reactors, as a rule of thumb, it can be assumed that the fraction of the gamma-energy absorbed in the fuel is equal to the ratio of the mass of the fuel to that of the core. In the thermal design of nuclear reactors, it can be assumed that 94% of the fission energy release takes place in the fuel. Table 7.2 give the distribution of the heat release among different components of CANDU reactors.

Table 7.2 Distribution of heat release among different components of CANDU reactors

Component	Released thermal energy, %
Energy released in the fuel	93.9
Energy released in the pressure tubes	0.3
Energy released in the calandria	0.1
Energy released in the coolant	0.5
Energy released in the moderator	5.0
Energy released in the shieldings	0.2
TOTAL	100.0

1.1.2 Volumetric Heat Generation Rate in Reactor Fuel

If we know the fission cross-section of the as a function of the neutron energy, $\sigma_f(E)$, the neutron flux as a function of the neutron energy and space, $\phi(\vec{r},E)$, and the number of fissile atoms per unit of volume, N_f, the volumetric heat generation rate in the reactor fuel is then given by:

$$q'''(\vec{r}) = \alpha E_R \int_0^\infty N_f \sigma_f(E) \phi(\vec{r},E) dE \qquad (7.1)$$

or representing $N_f\sigma_f(E)$ by $\Sigma_f(E)$ which is the macroscopic fission cross-section of the fuel, we can write:

$$q'''(\vec{r}) = \alpha E_R \int_0^\infty \Sigma_f(E) \phi(\vec{r},E) dE \qquad (7.2)$$

in Mev/cm^3; E_R is the recovered fission energy which is 200 Mev and α represents the portion of this energy deposited in the fuel. To express Eqs. 7.1 and 7.2 in W/cm^3 or in kW/m^3, they should be multiplied by $1.602x10^{-13}$ or $1.602x10^{-10}$, respectively. Defining the neutron flux weighted average of the fission cross-section of the fuel as:

$$\bar{\sigma}_f = \frac{\int_0^\infty \sigma_f(E)\phi(\vec{r},E)dE}{\int_0^\infty \phi(\vec{r},E)dE} \tag{7.3}$$

Eqs. 7.1 or 7.2 can be written as:

$$q'''(\vec{r}) = \alpha E_R N_f \bar{\sigma}_f \int_0^\infty \phi(\vec{r},E)dE = \alpha E_R \bar{\Sigma}_f \int_0^\infty \phi(\vec{r},E)dE. \tag{7.4}$$

In thermal reactors most of the fissions are induced by thermal neutrons. In this case, $\bar{\Sigma}_f$ is simply equal to the macroscopic fission cross-section of thermal neutrons and $\phi(\vec{r},E)$ is represented by $\phi(\vec{r})$ which is the thermal neutron flux. Therefore, Eq. 7.4 becomes:

$$q'''(\vec{r}) = \alpha E_R \bar{\Sigma}_f \phi(\vec{r}) \tag{7.5}$$

In the framework of a multigroup calculation, Eq. 7.2 is written as:

$$q'''(\vec{r}) = \alpha E_R \sum_n \Sigma_{fn}\phi_n(\vec{r}) \tag{7.6}$$

where n shows the number of groups and Σ_{fn} and $\phi_n(\vec{r})$ the macroscopic fission cross-section and neutron flux corresponding to each group respectively.

At this point it is useful to specify certain terms often used in nuclear engineering:

- *power density of the core:* thermal energy released per unit volume of the core, kW/lt or kW/m^3.
- *specific power of the fuel:* thermal energy released per unit mass of the fuel, kW/kg or MW/ton,
- *power density of the fuel:* thermal energy released per unit volume of the fuel, kW/lt or MW/m^3.

Table 7.3 gives the power densities for the most popular reactors.

1.1.3 Spatial Volumetric Heat Generation Distribution in the Reactor Core

Eq. 7.5 or 7.6 show that to determine the distribution of heat generation rate in the reactor, we need to know the distribution of the neutron flux throughout the region of the core which contains the fuel. The determination of an accurate neutron flux or power density distribution throughout the reactor core is a complicated process and usually requires the numerical solution

of multi-group diffusion or transport theory equations. Obviously the discussion of these procedures is beyond the scope of this course and they are dealt with in the reactor theory courses or text books. Within the scope of the present discussion, we will only consider cylindrical reactors

Table 7.3 Power density of popular reactors in MW/m^3

Reactor type	Average power density of the core	Average power density of the fuel*	Maximum power density of the fuel*
CANDU	12	110	190
Boiling water reactors	56	56	180
Pressurized water reactors	95-105	95-105	190-210
* Includes the coolant within the rod assemblies.			

with axial and radial reflectors. Furthermore, we will assume that fuel elements have a constant enrichment and are uniformly distributed throughout the core. This assumption allows us to treat the reactor core as homogeneous reactor and determine the over all features of the neutron flux distribution. Uniformly loaded pressurized water reactors fall in this category. In heavy water reactors where pressure tube design has been used (CANDU reactors), because of the substantial neutron flux depression in the fuel rod bundles contained in the pressure tubes, they can not be considered as homogeneous. However, we will still use the homogeneous reactor approach to get an idea on the overall neutron flux pattern.

Using a one group neutron approach, the thermal neutron flux distribution in the core region of a homogeneous reactor with radial and axial reflectors can be approximated by:

$$\phi = \phi_o J_o(2.405\frac{r}{R})\cos(\pi\frac{z}{H}) \tag{7.7}$$

where ϕ_o is the flux at the center of the reactor, J_o is the zero-order Bessel function of the first kind, r and z are the radial and axial coordinates and vary between 0 and R, and ½H and -½H, respectively. R and H are the radius and the height of the reactor core, and R' and H' are the effective radius and the height of the core including an allowance for the reflector. R and H are respectively smaller then R' and H'. Fig. 7a compare the variation of the thermal neutron flux in the radial direction determined with Eq. 7.7 and with the model of two neutron energy groups. We observe that Eq. 7.7 represents reasonably well the thermal neutron flux in the core region.

The average flux in the core region is given by:

$$\bar{\phi} = \frac{1}{\pi R^2 H}\int_0^R \int_{-\frac{H}{2}}^{\frac{H}{2}} \phi 2\pi\, r\, dr dz. \tag{7.8}$$

Substituting ϕ with Eq. 7.7 and carrying out the integration we obtain:

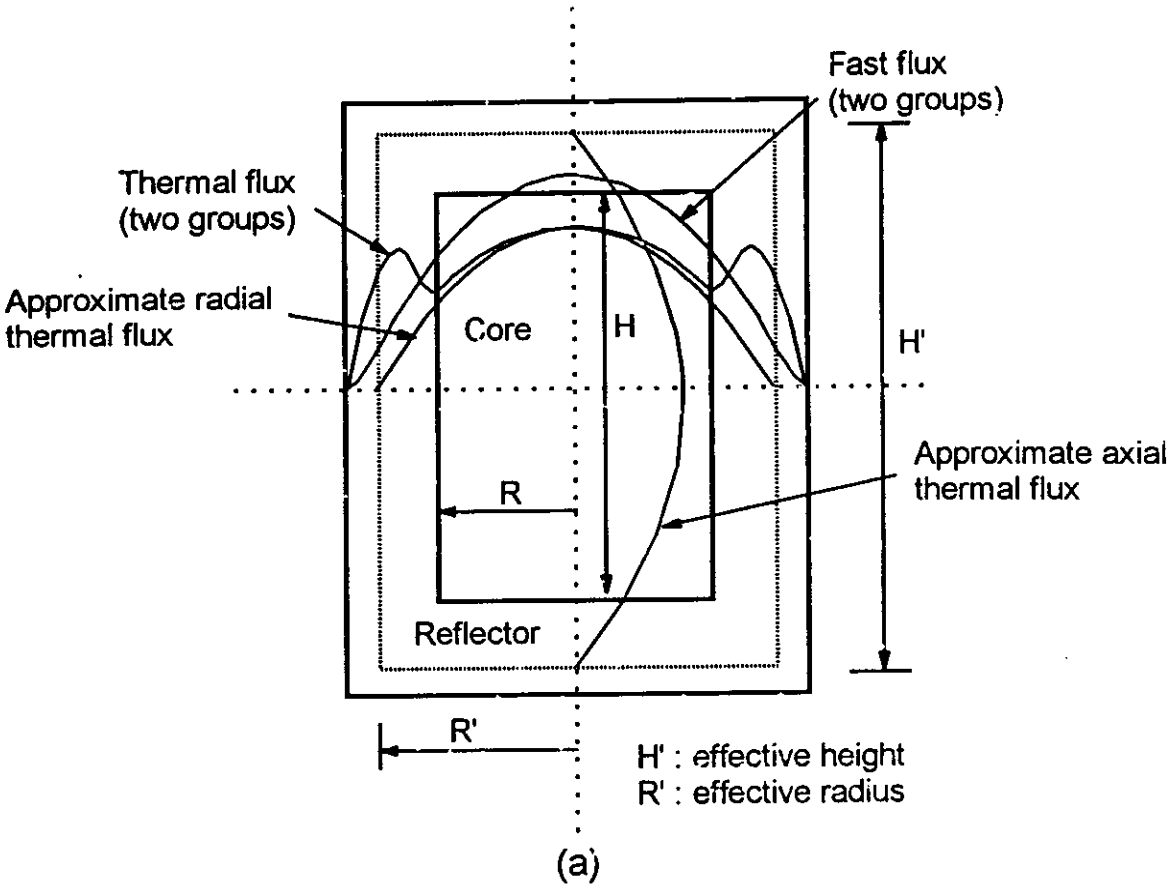

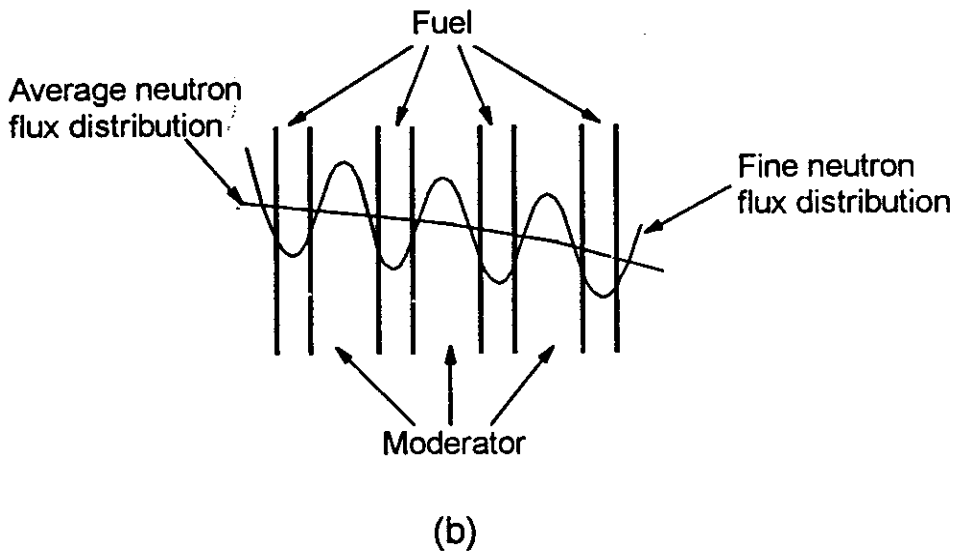

Figure 7.1 Comparison of radial thermal neutron distribution obtained with Eq. 7.7 and with two neutron energy groups

$$\frac{\bar{\phi}}{\phi_o} = \frac{2RR' J_1\left(2.405\frac{R}{R'}\right)}{2.405R^2} \cdot \frac{2H' \sin\left(\frac{\pi}{2}\frac{H}{H'}\right)}{\pi H} \tag{7.9}$$

where J_1 is the first order Bessel function. According to Eq. 7.5, the heat generation rate (or the power density of the core) is proportional to the thermal neutron flux. Therefore Eq. 7.9 also gives the ratio of the heat generation rate ,i.e., $\bar{q}'''/q_c'''$ where q_o''' is the maximum heat generation rate within the reactor. For a bare reactor where $R = R'$ and $H = H'$, the ratio given by Eq. 7.9 after inversion is:

$$\frac{q_o'''}{\bar{q}'''} = \frac{2.405}{2J_1(2.405)}\frac{\pi}{2} = 3.64 \tag{7.10}$$

For a reactor equipped with radial and axial reflectors, we can reasonably assume that:

$$\frac{R}{R'} = \frac{H}{H'} = 0.83 \ .$$

In this case the value of the $q_o'''/\bar{q}'''$ ratio is approximately 2.35. For a uniform radial neutron flux, the same ratio has the value of 1.57. These simple calculations show that the maximum neutron flux or heat generation rate in the core may be substantially higher than the average neutron flux or heat generation rate.

In reactor design, high $q_o'''/\bar{q}'''$ ratio is not desirable. In a given reactor, it may be possible to increase the power output by decreasing this ratio. In other words, the power output of the reactor can be increased by a more uniform distribution of the heat generation rate. This is usually referred to as "flattening of the heat generation distribution or of the neutron flux." The flattening of the neutron flux can be achieved by:

1. adding reflectors around a bare reactor,
2. varying radial fuel enrichment; however, exploitation problems prevents the use of any enrichment variation in the axial direction,
3. varying the ratio of fuel-to-moderator,
4. varying the extent of insertion of control rods, so that the neutron capture is greatest in these regions in which the flux would be otherwise high, or
5. using a neutron poison circulated as a solution in certain parts of the core.

The advantages of a neutron flux flattening are:

1. The power output of the reactor increases.

2. In a reactor with parallel channels, such as CANDU reactor, the distribution of the coolant to the channels can be easily achieved. In these reactors, orifices of different sizes are employed at the inlet of the channel in order to obtain a coolant flow rate which is proportional to the heat generated in that channel. The aim is to obtain the same coolant exit temperature and thus improve the efficiency of the steam cycle associated with the reactor.

1.1.4 Determination of The Maximum Neutron Flux

The value of the maximum thermal neutron flux, ϕ_o, appearing in Eq. 7.7 is not known a priori. A separate calculation using the total power of the reactor, $\mathbf{P}_t$, which is a design criterion, should be carried out. In practice, the total power for a non boiling reactor can be easily determined by measuring the flow rate of the coolant as well as its inlet and outlet temperatures to the reactor core. Let us determine now the maximum thermal neutron flux for a homogeneous reactor equipped with axial and radial reflectors.

Using Eqs. 7.5 and 7.7, we can write the total power of the reactor as:

$$\mathbf{P}_t = \int_{-\frac{1}{2}H}^{\frac{1}{2}H} \int_0^R q'''(r,z) 2\pi r dr dz = \alpha E_R \bar{\Sigma}_{fm} \int_{-\frac{1}{2}H}^{\frac{1}{2}H} \int_0^R \phi_o J_o(2.405 \frac{r}{R}) \cos \pi \frac{z}{H} 2\pi r dr dz \qquad (7.11)$$

where $\bar{\Sigma}_{fm}$ is the macroscopic fission cross-section of the mixture for the thermal neutrons. Since the reactor is homogeneous, we can assume that all the recovered fission energy, E_R, is deposited in the core, i.e., $\alpha \cong 1$. Knowing that:

$$\int r J_o(\lambda r) dr = \frac{r}{\lambda} J_1(\lambda r) \qquad (7.12)$$

we can easily integrate Eq. 7.11 and obtain:

$$\mathbf{P}_t = \phi_o E_R \bar{\Sigma}_{fm} \frac{RR'}{2.405} 4H' J_1\left(2.405 \frac{R}{R'}\right) \sin \frac{\pi}{2} \frac{H}{H'} \qquad (7.13)$$

or

$$\phi_o = \frac{\mathbf{P}_t}{E_R \bar{\Sigma}_{fm} \frac{RR'}{2.405} 4H' J_1\left(2.405 \frac{R}{R'}\right) \sin \frac{\pi}{2} \frac{H}{H'}}. \qquad (7.14)$$

Making the usual assumption for $R/R' = H/H' = 0.83$, Eq. 7.14 becomes:

$$\phi_o = 2.35 \frac{\mathbf{P}_t}{E_R \bar{\Sigma}_{fm} V} \qquad (7.15)$$

where V is the volume of the core. The same result could also be obtained from Eq. 7.9. For a reactor with axial and radial reflectors, we have found that:

$$\frac{\phi_o}{\bar{\phi}} = 2.35.$$

The total power of the reactor can be written as:

$$\mathbf{P}_t = \bar{\phi}\,\bar{\Sigma}_{fm} E_R V = \frac{\phi_o}{2.35}\,\bar{\Sigma}_{fm}\,E_R V \tag{7.16}$$

therefore,

$$\phi_o = 2.35\frac{\mathbf{P}_t}{E_R\,\bar{\Sigma}_{fm}\,V}$$

Substituting Eq. 7.15 into Eq. 7.7, we obtain the distribution of the thermal neutron flux:

$$\phi = \frac{2.35\mathbf{P}_t}{E_R\,\bar{\Sigma}_{fm}\,V} J_o\left(2.405\frac{r}{R}\right)\cos\pi\frac{z}{H} \tag{7.17}$$

The above equation can also be used to approximate the flux in a reactor which consists of fuel assemblies of n rods, provided that the value of $\bar{\Sigma}_{fm}$ is computed for an equivalent homogeneous mixture. Let us assume that there are N fuel assemblies in the reactor core and each assembly consists of n rods of fuel radius r_o and length H. Indicating by $\bar{\Sigma}_{fr}$ the macroscopic cross-section of the fuel, the total fission cross-section of the entire core is:

$$\bar{\Sigma}_{fr}\,Nn\pi\,r_o^2 H.$$

The average value of $\bar{\Sigma}_{fm}$ in the core is then given by:

$$\bar{\Sigma}_{fm} = \frac{\bar{\Sigma}_{fr}\,Nn\pi\,r_o^2 H}{\pi R^2 H} = \frac{\bar{\Sigma}_{fr}\,Nnr_o^2}{R^2}\,. \tag{7.18}$$

Substituting Eq. 7.18 into Eq. 7.17 we obtain:

$$\phi = 0.75\frac{\mathbf{P}_t}{E_R\,\bar{\Sigma}_{fr}\,Hr_o^2 Nn} J_o\left(2.405\frac{r}{R}\right)\cos\pi\frac{z}{H}\,. \tag{7.19}$$

It should be remembered that in heterogeneous reactors only a portion of the recoverable fission energy, α, is deposited in the fuel rod. The distribution of the heat sources in the reactor is obtained by introducing Eq. 7.19 into Eq. 7.5 and interpreting $\bar{\Sigma}_f$ as $\bar{\Sigma}_{fr}$:

$$q'''(r,z) = \frac{0.75\alpha\,\mathbf{P}_t}{Hr_o^2 Nn} J_o\left(2.405\frac{r}{R}\right)\cos\pi\frac{z}{H}\,. \tag{7.20}$$

This is the global distribution of the heat sources or power density in the reactor core. The dependence of q''' on r give the variation of the power density from rod assembly to rod assembly in the core not across any individual assembly nor across the fuel rod as illustrated in Fig. 7.1b. We assume that q''' is constant in a fuel assembly as well as in a fuel rod. Although this assumption is arguable for fuel assemblies, it does not introduce significant errors in the heat transfer calculations, especially for small diameter natural uranium or low enrichment fuel rods used in most power reactors.

1.2 Thermal Study of a Reactor Channel

As already pointed out, power reactors consist of fuel channels which contain natural or enriched fuel and pressurized high temperature coolant. The simplest arrangement is a single cylindrical fuel rod inserted in a circular cross-section channel. However, to achieve highest possible heat release from the reactor while maintaining the maximum fuel temperature below the permissible value, the heat transfer should be increased. For a given amount of fuel in the channel, the heat transfer surface may be increased either by dividing it into a number of small diameter rods, or by adding fins on the cladding of a single rod. The first solution is the one which is adopted by pressurized light and heavy water reactors, and boiling water reactors. In these reactors, the fuel is in the form of small-diameter rod bundles or assemblies. Adding fins on the cladding or subdividing the fuel into small-diameter rods has a negative effect on the neutron balance because of the increased neutron absorption.

1.2.1 Maximum and Average Linear Power of the Fuel Channel

For the neutron flux distribution we have selected, it is evident that the maximum power density is at the center of the core, i.e., $r = 0$ and $z = 0$. In this case, both functions in Eq. 7.20 are unity and the maximum value is:

$$q'''_{\max} = \frac{0.75\alpha P_t}{Hr_o^2 Nn}$$

and the power density distribution throughout the reactor can be written as:

$$q''' = q'''_{\max} J_o\left(2.405\frac{r}{R}\right)\cos\pi\frac{z}{H}. \tag{7.21}$$

From this equation, we can see that the power density distribution in a fuel channel located at a given radial distance is given by:

$$q''' = q'''_o \cos\pi\frac{z}{H} \tag{7.22}$$

where

$$q'''_o = q'''_{\max} J_o\left(2.405\frac{r}{R}\right). \tag{7.23}$$

It is more convenient to write Eq. 7.22 as:

$$q''' = q'''_o \cos 2\frac{\pi H}{2H'}\frac{z}{H} = q'''_o \cos 2\beta\frac{z}{H} \tag{7.24}$$

Using Eq. 7.24, the average power density in a fuel channel is written as:

$$q'''_{av} = \frac{\int_{-\frac{1}{2}H}^{\frac{1}{2}H} q'''_o \cos 2\beta\frac{z}{H}dz}{\int_{-\frac{1}{2}H}^{\frac{1}{2}H} dz} = q'''_o \frac{\sin\beta}{\beta} . \tag{7.25}$$

The linear power distribution along the channel is obtained by multiplying Eq. 7.24 by the cross section of the fuel:

$$q' = n\pi r_o^2 q'''_o \cos 2\beta\frac{z}{H} = q'_o \cos 2\beta\frac{z}{H} \tag{7.26}$$

where n is the number of the rods in the fuel assembly. The integration of Eq. 7.26 along the channel yields the total fuel channel power:

$$\mathbf{P}_c = \int_{-\frac{1}{2}H}^{\frac{1}{2}H} n\pi r_o^2 q'''_o \cos 2\beta\frac{z}{H}dz = \int_{-\frac{1}{2}H}^{\frac{1}{2}H} q'_o \cos 2\beta\frac{z}{H}dz = q'_o H\frac{\sin\beta}{\beta} . \tag{7.27}$$

Knowing that:

$$q'_{av} = q'_o \frac{\sin\beta}{\beta} \tag{7.28}$$

Eq. 7.27 can also be written as:

$$\mathbf{P}_c = Hq'_{av} \tag{7.29}$$

1.2.2 Basic Equations for the Thermal Study of a Fuel Channel

The basic equations for the thermal study of a fuel channel consist of the energy conservation equations applied to the coolant, to the cladding and to the fuel with appropriate boundary conditions. In order to determine the coolant energy conservation equation, let us consider a single fuel channel depicted in Fig. 7.2 and select a control volume which is laterally limited by the channel wall and fuel, and axially by planes at z and $z + dz$. The selection of a single fuel channel does not affect the generality of the approach. It can be easily extended to a multi-rod fuel bundle provided that a strong mixing takes place between the laterally interconnected subchannels bounded by the fuel rods or by the fuel rods and the channel wall. The application of energy conservation principle to the selected control volume yields:

$$\left(h + \frac{\partial h}{\partial z}dz\right) GA d\tau + \frac{\partial u}{\partial \tau} A\, dz\, \rho\, d\tau = hGA\, d\tau + q''_c s\, dz\, d\tau \tag{7.30}$$

or

$$\rho\frac{\partial u}{\partial \tau}+G\frac{\partial h}{\partial z}=\frac{q_c'' s}{A} \tag{7.31}$$

where:

q_c''	:	heat flux on the fuel element surface, kW/m²°C
A	:	channel flow area, m²
s	:	heated perimeter, m
ρ	:	fluid specific mass, kg/m³
u	:	specific internal energy, kJ/kg
h	:	specific enthalpy, kJ/kg
τ	:	time, s.

Assuming that the heat conduction in the axial and angular directions are negligible compared to that in the radial direction, the conduction equation derived in Chapter 1, yields the following equations for the fuel:

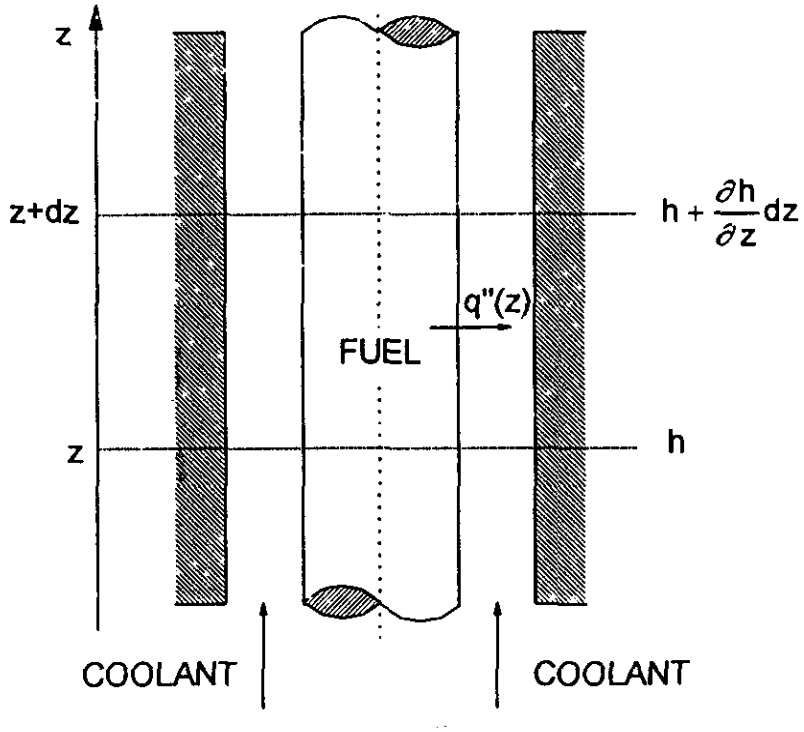

Figure 7.2 Fuel channel with single rod

$$\frac{1}{r}\frac{\partial}{\partial r}\left(k_f r\frac{\partial t}{\partial r}\right)+q'''=\frac{\partial}{\partial \tau}(\rho_f c_f t) \quad 0\le r\le r_o, \tag{7.32}$$

and the cladding:

$$\frac{1}{r}k_c\frac{\partial}{\partial r}\left(r\frac{\partial t}{\partial r}\right)=\frac{\partial}{\partial \tau}(\rho_c c_c t) \qquad r_o \le r \le r_c \tag{7.33}$$

where

k_f	:	conductivity of the fuel; usually a strong function of the temperature, W/m°C,
k_c	:	conductivity of the cladding; it may be taken as constant, W/m°C,
ρ	:	specific mass (f: fuel, c: cladding), kg/m^3,
c	:	specific heat, J/kg ,
$q^{'''}$	:	power density, W/m^3.

The boundary conditions are:

1. Inlet mass flow rate, kg/s.
2. Inlet temperature, °C.
3. Inlet pressure, Pa or MPa; as a first approximation, the pressure losses can be neglected beside the system pressure, this justifies the absence of the momentum conservation equation.
4. Heat convection at the fuel element surface:

$$-k_c\left(\frac{\partial t_c}{\partial r}\right)_{r=r_c}=h_c(t_c(r_c)-t) \tag{7.34}$$

where

h_c	:	convective heat transfer, W/m^2°C,
$t_c(r_c)$	:	temperature on the outer surface of the cladding , °C,
t	:	temperature of the coolant, °C,
r_c	:	radius of the fuel element, m.

5. Heat transfer at the fuel-cladding interface:

$$q'' = h_g(t_f(r_o)-t_c(r_o)) \tag{7.35}$$

where

h_g	:	gap conductance, W/m^2°C,
$t_f(r_o)$	:	temperature at the surface of the fuel, °C,
$t_c(r_o)$	:	temperature at the inner surface of the cladding, °C.

6. Continuity of the heat fluxes at the fuel-cladding interface:

$$k_f\left(\frac{\partial t_f}{\partial r}\right)_{r=r_o} = k_c\left(\frac{\partial t_c}{\partial r}\right)_{r=r_o} \tag{7.36}$$

The numerical solution of Eqs. 7.31,7.32 and 7.33 with the above boundary conditions and appropriate initial conditions yields the distribution of the coolant temperature in the axial direction and the distribution of the radial and axial temperatures in the fuel and the cladding. Although we have neglected the heat conduction in the axial direction, the variation of the temperature in the fuel and cladding in this direction is due to the variation of the coolant temperature and linear heat flux along the channel.

1.2.3 Coolant Temperature Along the Fuel Channel

Assuming steady state conditions, Eq. 7.31 can be written as:

$$GA\frac{dh}{dz} = q''_c s \tag{7.37}$$

or

$$\dot{m}\frac{dh}{dz} = q' \tag{7.38}$$

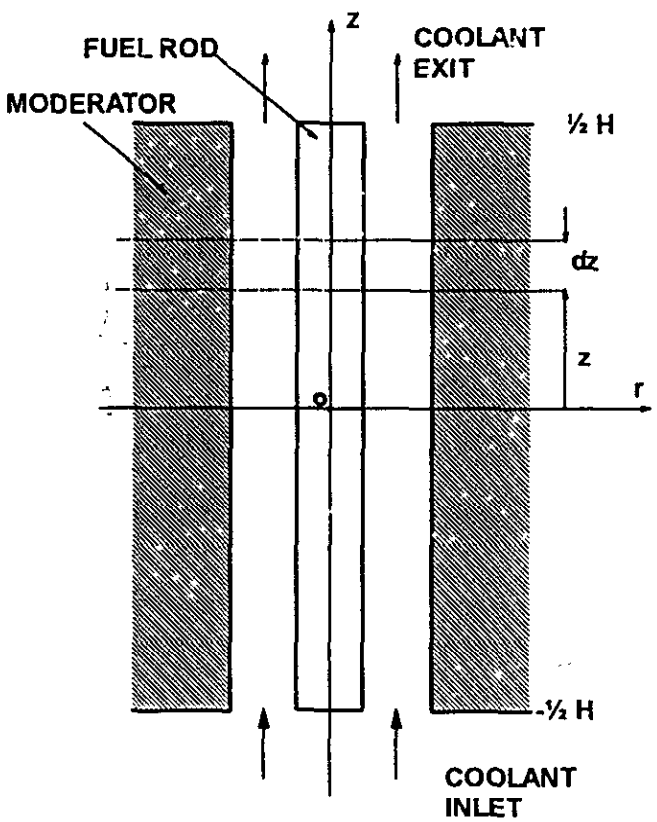

Figure 7.3 Fuel Channel
Figure 7.3 Fuel channel

where $\dot{m}$ is the mass flow rate and q' is the linear heat flux (or power density) whose variation along the channel is given by Eq. 7.26. Substituting q' in Eq. 7.38 by Eq. 7.26 and integrating the resulting equation between the inlet of the channel (located at $z = -\frac{1}{2}H$) and a given location z (Fig. 7.3) we obtain:

$$\dot{m}\int_{h_i}^{h} dh = \int_{-\frac{1}{2}H}^{z} q'_o \cos 2\beta \frac{z}{H} dz$$

or

$$h = h_i + \frac{q'_o}{\dot{m}} \frac{H}{2\beta} \sin\beta \left(\frac{\sin 2\beta \frac{z}{H}}{\sin\beta} + 1 \right) \tag{7.39}$$

The combination of Eq. 7.39 with Eq. 7.27 yields:

$$h = h_i + \frac{\mathbf{P}_c}{2\,\dot{m}} \left(\frac{\sin 2\beta \frac{z}{H}}{\sin\beta} + 1 \right). \tag{7.40}$$

Assuming that:

$$(h - h_i) \cong \bar{c}_p (t - t_i) \tag{7.41}$$

we can write Eq. 7.40 in the temperature form:

$$t = t_i + \frac{\mathbf{P}_c}{2\,\dot{m}\bar{c}_p} \left(\frac{\sin 2\beta \frac{z}{H}}{\sin\beta} + 1 \right) \tag{7.42}$$

or knowing that the total channel power is given by:

$$\mathbf{P}_c = \dot{m}\,(h_e - h_i) = \dot{m}\,\bar{c}_p (t_e - t_i \tag{7.43}$$

in the following form:

$$t = \frac{t_i + t_e}{2} + \frac{t_e - t_i}{2\sin\beta} \sin 2\beta \frac{z}{H} \tag{7.44}$$

where h_e and t_e are the coolant enthalpy and temperature at the channel exit, respectively.

Going back to Eq. 7.40 and subtracting from both sides the saturation enthalpy, h_f, and dividing both sides by the latent heat, h_{fg}, we obtain:

$$\frac{h - h_f}{h_{fg}} = \frac{h_i - h_f}{h_{fg}} + \frac{\mathbf{P}_c}{2\,\dot{m}\,h_{fg}} \left(\frac{\sin 2\beta \frac{z}{H}}{\sin\beta} + 1 \right). \tag{7.45}$$

Using the definition of the thermodynamic equilibrium quality, which is:

$$x = \frac{h - h_f}{h_{fg}}$$

we obtain the variation of the thermodynamic quality along the channel:

$$x = \frac{h_i - h_f}{h_{fg}} + \frac{\mathbf{P}_c}{2\,\dot{m}\,h_{fg}}\left(\frac{\sin 2\beta\frac{z}{H}}{\sin\beta} + 1\right). \tag{7.46}$$

For our application, x may have positive or negative values. The different values of x are interpreted as follows:

$x < 0$	:	subcooled liquid,
$x = 0$	:	saturated liquid,
$0 < x < 1$	:	saturated steam-water mixture,
$x = 1$	:	saturated steam,
$x > 1$	:	superheated steam.

1.2.4 Thermal Study of the Fuel Rod

The prediction of the behavior of a reactor core requires a sound knowledge of the temperature distribution throughout the fuel element during the steady state and transient conditions. In this section, the temperature distributions in the radial and axial directions in a cylindrical fuel element under steady state conditions will be discussed.

1.2.4.1 Temperature of the Cladding

The principal cladding material in light and heavy water power reactors is Zircaloy-4 which is an alloy of zirconium (98.38%), tin (1.3%), iron (0.22%) and chromium (0.10%). Stainless steel has also been used as cladding material. The major drawback of the stainless steel is its relatively high neutron absorption cross-section which requires an increase in the fuel enrichment. The stainless steel is not suitable for CANDU reactor where natural uranium is used as fuel. In turn, Zircaloy-4 has a very low neutron absorption cross-section compared to stainless steel and now is used as fuel element cladding in all light and heavy water cooled power reactors. Table 7.4 gives certain thermal properties of Zircaloy-4.

Table 7.4 Thermal Properties of Zircaloy-4

Density	Conductivity	Specific heat	Melting point	Limiting temperature
kg/m^3	W/mK (at °C)	J/kgK (at °C)	°C	°C
6570	12.7 (300)	328 (300)	1850	40
	13.1 (400)	357 (650)		

The temperature of the outside surface of the cladding is obtained by using the Newton cooling law given in Chapter xx:

$$t_c - t = \frac{q'}{h_c s} \tag{7.47}$$

where t_c is the outside temperature of the cladding, h_c is the heat transfer coefficient and s is the heated perimeter. Substituting Eqs. 7.44 and 7.26 into Eq. 7.47 and taking into account Eqs. 7.28 and 7.29, we obtain:

$$t_c = \frac{t_i + t_e}{2} + \frac{t_e - t_i}{2\sin\beta}\sin 2\beta\frac{z}{H} + \frac{1}{h_c s}\frac{\mathbf{P}_c}{H}\frac{\beta}{\sin\beta}\cos 2\beta\frac{z}{H} \tag{7.48}$$

or

$$t_c = \frac{t_i + t_e}{2} + \frac{t_e - t_i}{2\sin\beta}\left(\sin 2\beta\frac{z}{H} + \frac{1}{\gamma}\cos 2\beta\frac{z}{H}\right) \tag{7.49}$$

where we replaced the channel power $\mathbf{P}_c$ with Eq. 7.43 and called:

$$\gamma = \frac{h_c s H}{2\beta\, \dot{m}\, \bar{c}_p} \tag{7.50}$$

Eq. 7.49 gives the variation of the outside temperature of the cladding along the channel. This temperature has a maximum which can be determined by taking the derivative of Eq. 7.49 and equating it to zero:

$$\frac{dt_c}{dz} = \cos 2\beta\frac{z}{H} - \frac{1}{\gamma}\sin 2\beta\frac{z}{H} = 0$$

or

$$\gamma = \tan 2\beta\frac{z}{H}. \tag{7.51}$$

The maximum temperature is then located at:

$$z_m = \frac{H}{2\beta}\arctan\gamma \tag{7.52}$$

and has for value:

$$t_{c\max} = \frac{t_i + t_e}{2} + \frac{t_e - t_i}{2\sin\beta}\left[\sin(\arctan\gamma) + \frac{1}{\gamma}\cos(\arctan\gamma)\right]. \tag{7.53}$$

The maximum cladding temperature should be less then the maximum allowable temperature with a reasonable safety margin. The maximum allowable temperature for Zircaloy-4 cladding is 380 °C - 400 °C.

The temperature distribution in the cladding in the radial direction at a given axial location is determined by using Eq. 7.33. Assuming steady state conditions this equation becomes:

$$\frac{d}{dr}\left(r\frac{dt}{dr}\right)=0 \qquad \text{with } r_o < r < r_c \tag{7.54}$$

where, as already pointed out, heat conduction in the angular and axial directions are neglected compared to that in the radial direction. The integration of Eq. 7.54 yields:

$$t_c = A\ln r + B. \tag{7.55}$$

The constants A and B appearing in the above equation are determined by using ad hoc boundary conditions. In the present case, the inner surface of the cladding is subject to a constant linear heat flux, q' whereas the outer surface is kept at the temperature t_c, thus the boundary conditions can be written as:

$$r = r_o \qquad q' = -2\pi r_o k_c \frac{dt}{dr},$$

$$r = r_c \qquad t = t_c.$$

The constants A and B are evaluated as:

$$A = -\frac{q'}{2\pi k_c} \tag{7.56}$$

$$B = t_c + \frac{q'}{2\pi k_c}\ln r_c \tag{7.57}$$

and the variation of the temperature through the cladding is given by:

$$t = t_c + \frac{q'}{2\pi k_c}\ln\frac{r_c}{r} \qquad \text{with} \quad r_o \le r \le r_c. \tag{7.58}$$

The inner surface temperature of the cladding is obtained by setting $r = r_o$:

$$t_c' = t_c + \frac{q'}{2\pi k_c}\ln\frac{r_c}{r_o}. \tag{7.59}$$

1.2.4.2 Gap Conductance Between the Fuel and Cladding

Because of its low conductance for heat (or high resistance to heat flow) a large temperature drop, which is second to that in the ceramic fuel (UO_2) takes place in the gap region between the fuel and cladding. During the manufacturing of the fuel rods, a gap of about 0.08 mm is required between the outer surface of the fuel and the inner surface of the cladding in order to insert easily

the fuel pellets into the cladding tubes. In some reactors, such as CANDU, graphite powder has been used to facilitate the insertion of the fuel pellets. The cladding tubes are filled at atmospheric pressure, but in an atmosphere of an inert gas such as helium to avoid the corrosion and to assure a reasonable initial heat transfer. Since the gap between the surfaces is so small, the convection currents can not develop in the gas. Therefore, at an early stage, after the introduction of the fuel element into reactor, the heat transfer in the gap region is by conduction through the filling gas. Latter, because of the swelling and thermal expansion of the fuel which is more important than that of the cladding, the gap region closes and direct contact between the surfaces at several discrete points takes place. Consequently, the heat transfer by conduction at these points should be taken into account when modeling the heat transfer through the gap region.

The gap heat transfer are usually expressed in terms of a gap heat transfer coefficient or conductance, h_g. If the temperature on the fuel surface and on the inner surface of the cladding are t_f and t'_c, respectively, then the linear heat flux across the gap is:

$$q' = 2\pi r_o h_g \left(t_f - t'_c\right) . \tag{7.60}$$

Based on the above arguments, the modeling of the gap heat transfer coefficient (gap conductance) will be conducted for two general cases that exist: open and closed gaps.

1. Open gap

If the fuel and cladding is not in physical contact, which is true for fresh fuel or fuel operating at very low linear power rate, the fuel stands freely within the cladding. In such a case, the heat transfer mechanisms are conduction through the filling gas and radiation. At the insertion of the fuel into reactor, the filling gas, as already pointed out, is pure helium close to atmospheric pressure. After staying in the reactor for long period of time, the fission product gases such as krypton and xenon released from fuel start filling the gap region and mixing with the helium. The accumulation of the gas in the gap region increases the pressure in this region, i.e., the pressure within the fuel element. Towards the end of the fuel life in the reactor, this pressure can be as high as 7.5 MPa and the gas that conducts the heat from fuel to cladding is a mixture of helium, krypton (~15%) and xenon (~85%).

If the space between the fuel and the cladding is much larger than the mean free path of the atoms at the prevailing temperature and pressure, the gap conductance, taking also into account the heat exchange by radiation between the exposed surfaces, is given by:

$$h_g = \frac{k_g}{\delta_g} + \frac{\sigma}{\frac{1}{\varepsilon_f} + \frac{1}{\varepsilon_c} - 1} \frac{T_f^4 - T_c'^4}{T_f - T_c} \tag{7.61}$$

where k_g is the thermal conductivity of the gas, δ_g is the gap thickness, σ is the Stefan-Boltzman constant, and ε_f and ε_c are the surface emissivities of the fuel and cladding, respectively. For small gaps where a temperature gradient is also sustained, a steep change in the gas temperature is observed in the regions close to the solid surfaces. The variation of the gas temperature in the gap region is illustrated in Fig. 7.4. This steep change takes place within a mean free path from the

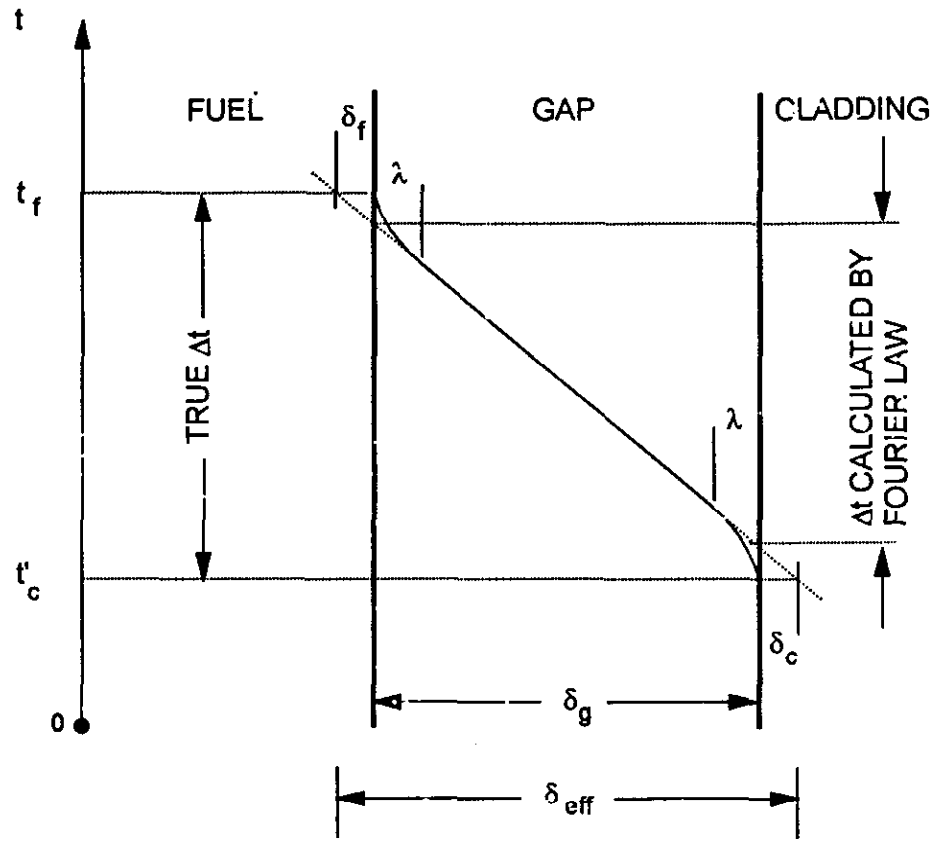

Figure 7.4 Temperature profile in the gap region and temperature jump

walls and is called "the temperature jump." From the figure it can be seen that the extrapolation of the temperature profile in the bulk of the gas intersects the fuel and the cladding temperature in the solids at distances δ_f and δ_c, respectively. These distances are called "*temperature jump distances*" and should be added to the actual gap thickness in order to predict the correct fuel-cladding temperature difference by using the Fourier conduction law. The conductance for narrow gaps (few mean free path) is then given by:

$$h_g = \frac{k_g}{\delta_g + \delta_f + \delta_c} + \frac{\sigma}{\frac{1}{\varepsilon_f} + \frac{1}{\varepsilon_c} - 1} \frac{T_f^4 - T_c'^4}{T_f - T_c'} \tag{7.62}$$

Kennard (1938) gives the temperature jump distance as:

$$\delta = 2\left(\frac{2-\alpha}{\alpha}\right)\left(\frac{\Gamma}{1-\Gamma}\right)\left(\frac{k}{\mu c_p}\right)_g \lambda \tag{7.63}$$

where

λ : mean free path in the gas

Γ	:	ratio of c_p /c_v for the gas
c_p	:	specific heat at constant pressure
c_v	:	specific heat at constant volume
μ	:	viscosity of the gas
k	:	conductivity of the gas

The quantity α in Eq. 7.63 is called thermal accommodation coefficient of the gas in contact with a solid surface. This coefficient takes into account the incomplete energy interchange between the gas molecules and the solid surface, and is given by:

$$\alpha = \frac{T_r - T_i}{T_s - T_i} \tag{7.64}$$

where, T_i is the temperature of molecules that strikes the solid, T_s is the temperature of the solid and T_r is the temperature of the reflected molecules. α is usually less than 1; when it is equal to unity, the reflected molecules are perfectly in equilibrium with the solid. It is interesting to note that the roughness of the solid surface increases the value of the thermal accommodation coefficient by making possible multiple collisions of an impinging gas atom with the solid before the former escapes from the surface.

The mean free path appearing in Eq. 7.63 is given by:

$$\lambda = \frac{\lambda_o}{p}\frac{T}{273} \tag{7.65}$$

where T is the absolute temperature in Kelvin, p gas pressure in bar and λ_o is the property of the gas that depends on the molecular or atomic diameter. For helium λ_o=1.74x10^{-5} bar-cm and for xenon λ_o=3.6x10^{-6} bar-cm. The mean free path in helium at 1 bar pressure and at room temperature is 0.2 μm; for xenon at 10 bars pressure and 1000 K the mean free path is 0.01 μm. For a fresh fuel, the gap width is typically ~80 μm. Consequently, δ_f and δ_c, which are in the order of magnitude mean free path, can be neglected in comparison with the gap thickness until the gap closes and the solids make contact.

The radiation component of the gap conductance appearing in Eq. 7.62 is usually small under normal operating conditions. Therefore, this component can be neglected in comparison with the conduction component and for small gap Eq. 7.62 takes the following form:

$$h_g = \frac{k_g}{\delta_g + \delta_f + \delta_c} \,. \tag{7.66}$$

Kampf and Karsten (1970) gave the following relationship of the conductivity of the pure gases:

$$k_g = A \cdot 10^{-6} T^{0.79} \quad W/cmK \tag{7.67}$$

where T is the average gas temperature in the gap in Kelvin and A is a constant and is equal to 15.8 for helium, 1.97 for argon, 1.15 for krypton and 0.72 for xenon. The thermal conductivity of a mixture of two gases that develops in the gap region as a result of release of fission gases from the fuel is approximated by (Kampf and Karsten, 1970):

$$k_g = (k_1)^{x_1}(k_2)^{1-x_2} \tag{7.68}$$

where k_1 and k_2 are the conductivity of the gases and x_1 and x_2 are the mole fractions of the same gases.

2. Closed gap

In practice, because of the fuel swelling, differential expansion of the fuel and the pressure exerted by the coolant on the outside surface of the cladding the gap tends to close. In turn, the pressure built-up in the region because of the accumulation of the fission gases and fuel diameter reduction due to the fuel densification the gap tends to open. However, the effects which try to close the gap are much more important than those which try to open the gap. Consequently, the gap thickness will be considerably reduced and because of the roughness of the fuel and cladding surfaces, solid-to-solid contact between them will be established at high points. Under this condition, heat transfer in the gap region occurs through the points of solid contact and across the now discontinuous gas gap between these points of contact. Fig. 7.5 depicts how the closed gap may look like.

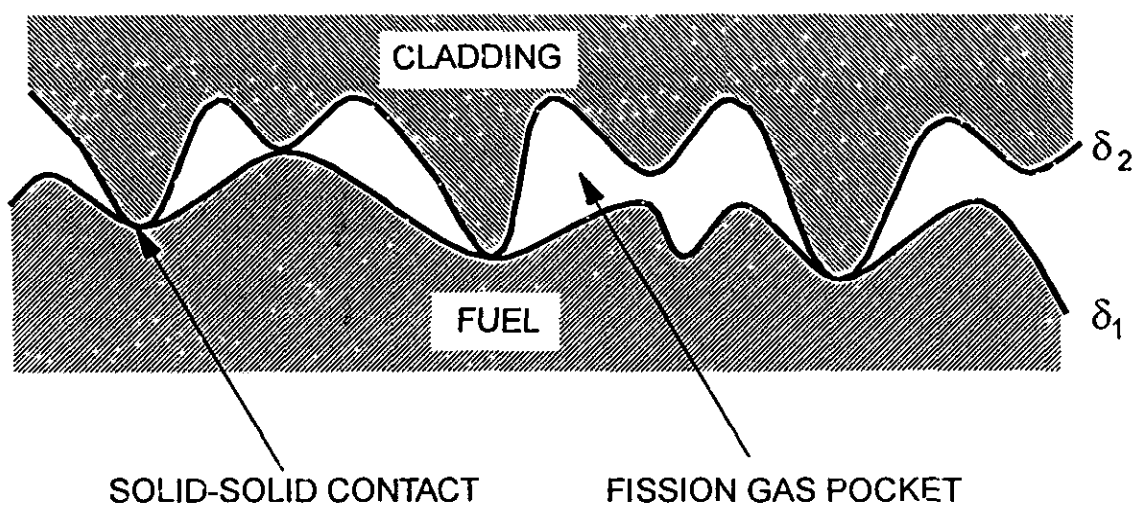

Figure 7.5 Closed fuel-cladding gap

For a closed gap, different components of the conductance are:

1. Gas conductance through discontinuous gap, h_g.
2. Conduction through the solid-to-solid contact points, h_s.
3. Radiation through the discontinuous gap, h_r.

Based on the work of Cetinkale and Fisherden (1951), Ross and Stout (1962) gave for the conductance due to solid-to-solid contact the following relationship:

$$h_s = A\frac{2k_f k_c}{k_f + k_c}\frac{p_i}{H\delta^{\frac{1}{2}}} \tag{7.69}$$

where

A	:	dimensional constant, $m^{½}$ (=10 $m^{½}$),
k_f	:	conductivity of the fuel, W/m°C,
k_c	:	conductivity of the cladding, W/m°C,
p_i	:	surface contact pressure, N/m^2,
H	:	Meyer hardness number of the softer material, N/m^2
δ	:	root-mean-square of contact material surface roughness and given by:

$$\delta = \left[\left(\delta_1^2 + \delta_2^2\right)/2\right]^{\frac{1}{2}},\ m,$$

δ_1,δ_2	:	surface roughness of the interface material, m.

Ross and Stout (1962) assumed that the thickness of a closed gap is related to the surface roughness as:

$$\delta_g = C(\delta_1 + \delta_2) \tag{7.70}$$

where C is a constant which depends on the interface pressure; they proposed the following correlation for this constant:

$$C = 2.75 - 2.55x10^{-8}p_i \tag{7.71}$$

where p_i is the pressure at the interface in N/m^2. Substituting Eq. 7.70 into Eq. 7.62 and neglecting the radiation, the authors obtained:

$$h_g = \frac{k_g}{C(\delta_1 + \delta_2) + \delta_f + \delta_c}. \tag{7.72}$$

Ross and Stout (1962) estimated the values of $(\delta_f + \delta_c)$ for various gases by comparing the analysis with experimental data. These values for different gases are listed in Table 7.5.

Table 7.5 Temperature jump distances for various gases (Ross and Stoute, 1962)

Gas	$\delta_f+\delta_c$, m	Temperature range, °C
Helium	$10x10^{-6}$	150-250
Argon	$5x10^{-6}$	180-320
Krypton	$1x10^{-6}$	180-330
Xenon	$1x10^{-6}$	180-330

The total conductance, h_{con}, of a closed gap is obtained by adding Eqs. 7.69 and 7.72, and taking into account heat exchanges by radiation (if required) between the fuel and cladding:

$$h_{con} = A\frac{2k_f k_c}{k_f + k_c}\frac{p_i}{H\delta^{\frac{1}{2}}} + \frac{k_g}{C(\delta_1+\delta_2)+\delta_f+\delta_c} + \frac{\sigma}{\frac{1}{\varepsilon_f}+\frac{1}{\varepsilon_c}-1}\frac{T_f^4 - T_c'^4}{T_f - T_c'}. \qquad (7.73)$$

Under normal operating conditions, the radiation component of the gap conductance can be ignored.

1.2.4.3 Surface Temperature of the Fuel

Combining Eqs. 7.59 and 7.60, we obtain the surface temperature of the fuel the following expression:

$$t_f = t_c + \frac{q'}{2\pi k_c}\ln\frac{r_c}{r_o} + \frac{q'}{2\pi r_o h_{con}}. \qquad (7.74)$$

The variation of t_c is given by Eq. 7.49; replacing this equation into the above equation and taking into consideration Eqs 7.26 and 7.27, we obtain:

$$t_f = \frac{t_i + t_e}{2} + \frac{t_e - t_i}{2\sin\beta}\left[\sin 2\beta\frac{z}{H} + \left(\frac{1}{\gamma} + \frac{\beta}{\pi k_c}\frac{\mathbf{P}_c}{(t_e - t_i)H}\ln\frac{r_c}{r_o}\right.\right.$$

$$\left.\left. + \frac{\beta}{\pi r_o h_{con}}\frac{\mathbf{P}_c}{(t_e - t_i)H}\right)\cos 2\beta\frac{z}{H}\right] \qquad (7.75)$$

or calling:

$$\frac{1}{\gamma'} = \frac{1}{\gamma} + \frac{\beta}{\pi k_c}\frac{\mathbf{P}_c}{(t_e - t_i)H}\ln\frac{r_c}{r_o} + \frac{\beta}{\pi r_o h_{con}}\frac{\mathbf{P}_c}{(t_e - t_i)H} \qquad (7.76)$$

we can write Eq. 7.76 as:

$$t_f = \frac{t_i + t_e}{2} + \frac{t_e - t_i}{2\sin\beta}\left(\sin 2\beta\frac{z}{H} + \frac{1}{\gamma'}\cos 2\beta\frac{z}{H}\right). \qquad (7.77)$$

The location of the maximum temperature can be easily found by deriving Eq. 7.77 with respect to z:

$$\frac{\partial t_f}{\partial z} = \cos 2\beta\frac{z}{H} - \frac{1}{\gamma'}\sin 2\beta\frac{z}{H} = 0 \qquad (7.78)$$

or

$$z_m = \frac{H}{2\beta}\arctan\gamma'. \qquad (7.79)$$

Substituting Eq. 7.79 into Eq. 7.77, we obtain the maximum temperature as:

$$t_{f\max} = \frac{t_e + t_i}{2} + \frac{t_e - t_i}{2\sin\beta}\left[\sin\left(\arctan\gamma'\right) + \frac{1}{\gamma'}\cos\left(\arctan\gamma'\right)\right]. \tag{7.80}$$

Calling $X = \arctan\gamma'$ and knowing that $\gamma' = \tan X$, we can write Eq. 7.80 as:

$$t_{f\max} = \frac{t_i + t_e}{2} + \frac{t_e - t_i}{2\sin\beta}\left(\sin X + \frac{1}{\tan X}\cos X\right) \tag{7.81}$$

or using the trigonometric relationship:

$$\sin X = \frac{\tan X}{\sqrt{1+\tan^2 X}} \tag{7.82}$$

as

$$t_{f\max} = \frac{t_i + t_e}{2} + \frac{t_e - t_i}{2\sin\beta}\sqrt{1+\left(\frac{1}{\gamma'}\right)^2}. \tag{7.83}$$

An examination of the above equation in conjunction with Eqs. 7.50 and 7.76 shows that the t_{fmax} decrease with increasing convective heat transfer coefficient and gap conductance. .

1.2.4.4 Temperature Distribution in the Fuel

We will now determine the radial temperature distribution in the fuel and discuss the variation of the fuel centerline temperature along the channel. In the determination of the radial temperature distribution, we will make the following assumptions:

1. The neutron flux is uniform within the fuel pellet, therefore, the heat generation rate also can be assumed as uniform; latter we will also discuss the case where there is a neutron flux depression within the fuel.
2. There is no angular variation in the convective heat transfer coefficient and gap conductance; therefore, no significant angular temperature gradient exists in the fuel.
3. The axial conduction of heat is small compared to that in the radial direction; since length to diameter ratio is usually higher than 20, this assumption is quite reasonable.
4. The steady state conditions prevail.

Under the above conditions, the heat conduction equation (Eq. 7.32) can be written as:

$$\frac{1}{r}\left(\frac{d}{dr}k_f r\frac{dt}{dr}\right) + q''' = 0. \tag{7.84}$$

Integrating once the above equation we get:

$$k_f r\frac{dt}{dr}+q'''\frac{r^2}{2}+A=0 \tag{7.85}$$

or

$$k_f\frac{dt}{dr}+q'''\frac{r}{2}+\frac{A}{r}=0. \tag{7.86}$$

Let us assume that the fuel has an internal cavity of radius r_i which is not cooled. Therefore, there is no heat flux at r_i and the corresponding boundary condition is written as:

$$q''_{r=r_i}=-k_f\frac{dt}{dr}\bigg|_{r=r_i}=0. \tag{7.87}$$

Using this boundary condition, the constant A in Eq. 7.86 can be easily determined:

$$A=-\frac{q'''r_i^2}{2}. \tag{7.88}$$

The integration of Eq. 7.86 between r and r_o, which is the outside fuel diameter, yields:

$$\int_t^{t_f}k_f dt=-\frac{q'''}{4}\left(r_o^2-r^2\right)+\frac{q'''}{2}r_i^2\ln\frac{r_o}{r} \tag{7.89}$$

or

$$\int_{t_f}^{t}k_f dt=\frac{q'''r_o^2}{4}\left[1-\left(\frac{r}{r_o}\right)^2-\left(\frac{r_i}{r_o}\right)^2\ln\left(\frac{r_o}{r}\right)^2\right]. \tag{7.90}$$

For a fuel pellet where $r_i=0$, Eq. 7.90 becomes:

$$\int_{t_f}^{t}k_f dt=\frac{q'''r_o^2}{4}\left[1-\left(\frac{r}{r_o}\right)^2\right]. \tag{7.91}$$

A relationship between the temperature at the center (t_o), at the surface (t_f) and the radius of the fuel can be obtained by setting in Eq. 7.91 $r=0$:

$$\int_{t_f}^{t_o}k_f dt=\frac{q'''r_o^2}{4}; \tag{7.92}$$

this equation can also be written as:

$$\int_{t_f}^{t_o}k_f dt=\frac{q'}{4\pi} \tag{7.93}$$

where q' is the linear power (or heat flux) which is given by:

$$q'=\pi r_o^2 q'''$$

It is interesting to note that the temperature difference across the solid fuel pellet is fixed by the linear heat flux and independent of the pellet radius. Thus a limit on the linear heat flux is directly imposed by a design requirement on the maximum temperature. The integral on the left of Eq. 7.93 is called *"the conductivity integral."* It is particularly useful when the conductivity varies substantially with temperature; its utility is due to the following properties:

1. It is directly related to the linear power of the fuel which can be determined by coolant calorimetric or post irradiation burnup analysis.
2. The central temperature of the rod, which is the upper limit of the conductivity integral, is independent of the rod diameter.
3. The upper limit of the conductivity integral can be taken as a variable, the differentiation yields the thermal conductivity.
4. By addition, the conductivity integral can be normalized to any temperature as the lower limit of integration; thus, normalized to 0 °C, it becomes:

$$\int_{t_f}^{t_o} k_f dt = \int_0^{t_o} k_f dt - \int_0^{t_f} k_f dt \qquad (7.94)$$

5. For design purposes, the integral can be used to estimate the centerline temperature of the fuel for specified power conditions.

I. Metallic fuels

Uranium metal is a very poor reactor fuel; it shows substantial dimensional changes under irradiation and thermal cycling. Highly irradiated fuel rod may show an axial growth as high as 60 % of its original length. This dimensional instability is due to the properties of the α phase, which is present below 665 °C. The α phase is anisotropic, consequently under irradiation and thermal cycling, the uranium rod will display substantial expansion in the axial direction and contraction in the radial direction. Because of this dimensional instability, the cladding may fail and the fuel is exposed to the coolant. Uranium metal is highly reactive chemically with light and heavy water. Exposure of the failed fuel to water at 290 °C for few hours will completely destroy the fuel element. However, uranium metal is compatible with gas coolants such as carbon dioxide and helium. Alloying materials such as Zr, Cr, Mo, Fe, etc. are capable of limiting the dimensional instability but they are often found to cause excessive parasitic neutron capture, especially for thermal neutrons. For the above reasons, uranium metal fuel or its alloys are not used in PWR, BWR and CANDU reactors. However, metal uranium and its alloys are used in low temperature and in gas cooled reactors

The conductivity of metal uranium as well as its alloys vary with temperature. Table 7.5 gives the conductivity of metal uranium as well as the conductivity of uranium dioxide and uranium carbide. We observe that the conductivity of metal uranium varies moderately between 100 °C and 750 °C. Therefore in the determination of the fuel temperature distribution, we can assume that the conductivity is constant and use a reasonable average value. The conductivity of the pure metal uranium as a function of temperature in °C is given by:

$$k_f = 25.58 + 1.75\left(\frac{t}{100}\right) + 0.018\left(\frac{t}{100}\right)^3 \text{ in W/m °C} \tag{7.95}$$

and for an alloy of U-Mo at 1% by

$$k_f = 22.4 + 2.3\left(\frac{t}{100}\right) + 0.015\left(\frac{t}{100}\right)^3 \text{ in W/m °C} \tag{7.96}$$

Table 7.6 Conductivity of fuel materials

Température °F	Uranium	UO_2	Thorium	ThO_2	UC
	K_c = Btu/hr pd °F				
200	15.80	4.5	21.75	7.29	14.77
300	16.40	-	22.18	6.25	14.07
400	17.00	3.5	22.60	5.34	13.48
500	17.50	-	23.00	4.61	13.02
600	18.10	2.8	23.45	4.03	12.67
700	18.62	-	23.90	3.59	12.39
800	19.20	2.5	24.30	3.21	12.19
900	19.70	-	24.65	2.91	12.02
1 000	20.25	2.2	25.75	2.68	11.91
1 100	20.75	-	25.60	2.47	
1 200	21.20	2.0	26.13	2.30	11.82
1 300	21.60	-	-	2.17	
1 400	22.00	1.6	-	2.07	11.76
1 600	-	1.5	-	1.90	11.70
1 800	-	1.4	-	1.80	11.67
2 000	-	1.3	-	1.70	11.57
2 200	-	1.2	-	1.69	-
2 400	-	1.1	-	1.68	-
2 600	-	1.1	-	-	-
3 200	-	1.1	-	-	-

For a constant conductivity, Eq. 7.91 can be easily integrated to obtain the radial temperature distribution in the fuel:

$$t = t_f + \frac{q'}{4\pi k_f}\left[1 - \left(\frac{r}{r_o}\right)^2\right] \tag{7.97}$$

The centerline temperature of the fuel is obtained by setting $r = 0$:

$$t_o = t_f + \frac{q'}{4\pi k_f}. \tag{7.98}$$

In turn, using Eqs. 7.26, 7.28, 7.29 and 7.77, we obtain the variation of the center line temperature along the channel as:

$$t_o = \frac{t_i + t_e}{2} + \frac{t_e - t_i}{2\sin\beta}\left(\sin 2\beta\frac{z}{H} + \frac{1}{\gamma''}\cos 2\beta\frac{z}{H}\right) \tag{7.99}$$

where

$$\frac{1}{\gamma''} = \frac{1}{\gamma'} + \frac{\beta}{2\pi k_f}\frac{\mathbf{P}_c}{(t_e - t_i)H}. \tag{7.100}$$

The maximum centerline temperature is located at

$$z_{\max} = \frac{H}{2\beta}\arctan\gamma'' \tag{7.101}$$

and the value of this maximum is:

$$t_{o\max} = \frac{t_i + t_e}{2\sin\beta} + \frac{t_e - t_i}{2\sin\beta}\sqrt{1 + \left(\frac{1}{\gamma''}\right)^2}. \tag{7.102}$$

II. Ceramic fuels

Uranium dioxide, a ceramic material, is used as fuel in commercial power reactors because of its dimensional stability, adequate resistance to radiation and high melting point. In addition, uranium dioxide does not react chemically with hot light or heavy water. It is the latter property which makes the uranium dioxide attractive as fuel in water-cooled reactors. Uranium dioxide retains also a large portion of the fission gases as long as its temperature is less 1000 °C. The major disadvantage of uranium dioxide is its low conductivity which causes high temperature gradients in the fuel (in the order of magnitude of 10^6 °C/m) and high centerline temperature (between 2000 and 2400 °C). The melting temperature of uranium dioxide is approximately 2800 °C.

As already pointed out, the cylindrical fuel pellets are manufactured by compacting under high pressure a finely ground UO_2 powder. The pellets are then sintered in a neutral or reducing atmosphere (to avoid the oxygen uptake) at a temperature of about 1700 °C for a predetermined length of time to increase the density. By controlling the sintering conditions, material of any desired density between 80% and 98% of the theoretical density can be produced; usually the density of the pellet is about 90% of the theoretical density. The pellets, after grinding to specified dimensions, are inserted into a zircalloy tubing and sealed by welding the end cap.

During irradiation, under the effect of high temperature and temperature gradients, sintered uranium dioxide fuel pellets undergo significant alterations in the morphology. These high temperatures and gradients produce a rapid diffusion of the oxides toward the low temperature region of the pellets and reciprocating movement of the voids (or pores of the sintered material) toward the high temperature region, i.e., toward the center. The result is the restructuring of the fuel pellet in characteristic zones: columnar grains, equiaxed grains and unchanged fuel, and possibly the formation of a central circular void as shown in Fig. 7.6. In the "*unchanged region*" where the tem-

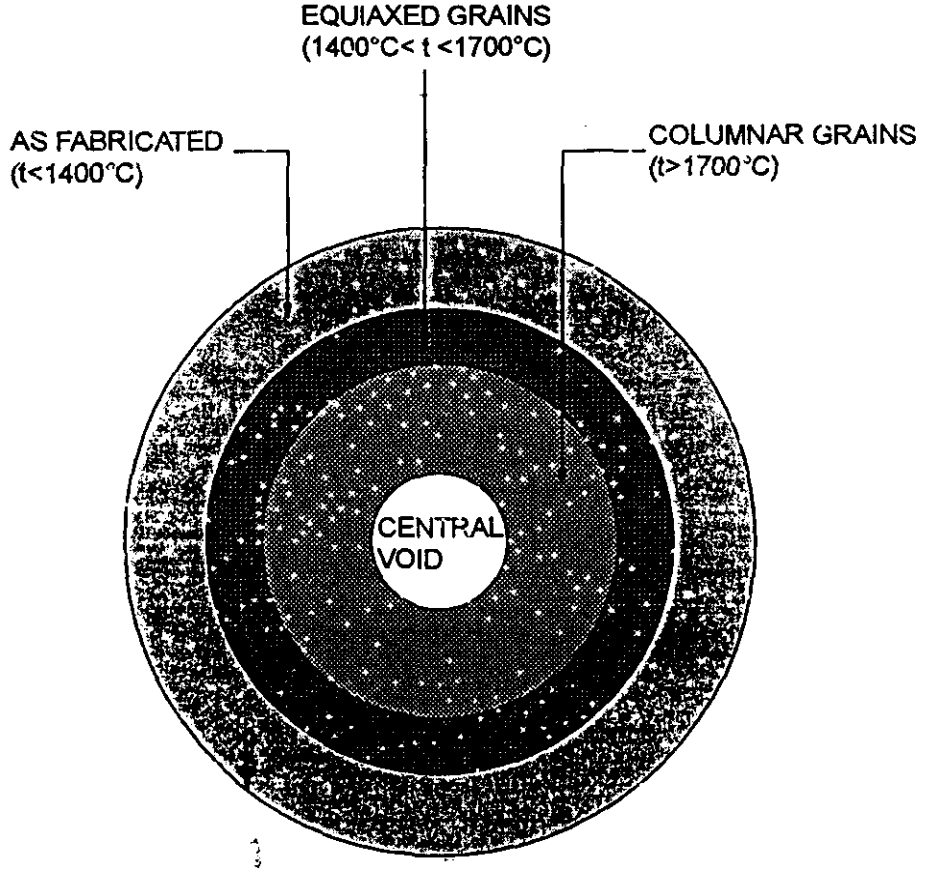

Figure 7.6 Restructuring of an oxide fuel pellet during the high temperature irradiation

peratures are too low to cause any restructuring, the fuel keeps, practically, its initial fine grain structure. Moving inward from the unchanged region, we find a band of equiaxed grains. In this region, the temperature (that is above the sintering temperature) rather than the temperature gradient is the significant parameter. In this zone, the initial fine grains of the as fabricated oxides grow many times of their original size and "*equiaxed grains*" with a random orientation are formed. Nearer the center, where the thermal gradient is large, there is a region characterized by large *columnar grains*. The boundaries of these grains are delineated by fine radial streaks. The radial boundaries of the columnar grains are the trails of the pores present in the as-fabricated fuel material or fission gas bubbles that migrated up to the temperature gradient. In the normal operation of water cooled reactors only equiaxed growth has been observed. However, under high

power ratings as in the fast reactors, the fuel restructuring is more extensive and all the above described regions, including the central void have been observed.

Besides the fuel restructuring , the large thermal gradients lead to thermal stesses. In turn, these stresses lead to radial cracking of the pellets during operation. However, the cracking does not seem to cause any significant deterioration in fuel performance provided that the pellets are suitably restrained by the cladding. One of the main limitation on the performance of uranium dioxide fuel is the swelling caused by the formation of two fission product atoms for every fissile atom destroyed and mainly by the gaseous fission products. At low and moderate burnups, the swelling is not significant and varies roughly linearly with burnup. Above a critical burnup, the swelling increases markedly and continued exposure of the fuel leads to unacceptable dimensional changes. The critical burnup can be increased by using slightly less dense uranium dioxide or by providing more cladding restraint. The critical burnup for unrestrained uranium dioxide at normal PWR operating conditions is shown in Fig. 7.7 as a function of the void (pore population) within the fuel (Tong, 1967). This figure clearly shows that the critical burnup increases with decreasing fuel density (or increasing void). A value of about $17x10^3$ MWd/tonne is obtained with a fuel of 97% of the theoretical density, and a value of $42x10^3$ MWd/tonne results for a value of 93% of the

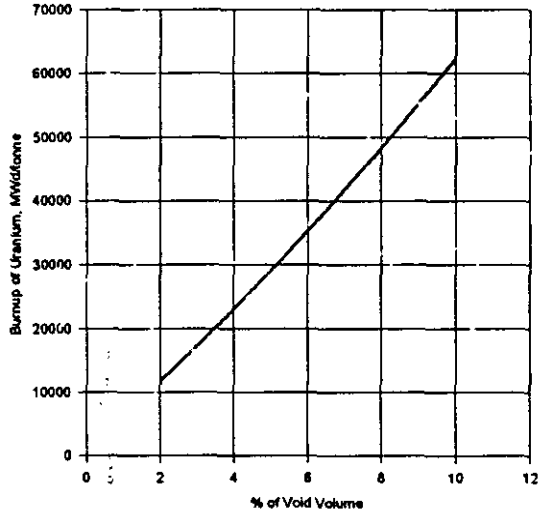

Figure 7.7 Effect of the void within the fuel on the critical burnup

theoretical fuel density. The theoretical density is the density of a poreless solid. The critical burnup also depends on the operating temperature of the fuel.

Thermal conductivity of uranium dioxide

Because of the wide use of uranium dioxide as reactor fuel, its properties in general and its conductivity in particular have been subject to numerous investigations. Despite these investigations, the thermal conductivity of uranium dioxide is not known with a satisfactory accuracy. It is observed that the conductivity of the ceramic fuels depends on the temperature, on the porosity and on the burnup.

As already discussed, the oxide fuel is fabricated by sintering pressed uranium dioxide powder at high temperature. By controlling the sintering conditions, material at a density usually around 95% of the maximum possible or theoretical density of the solid is produced. This means that the 5% of the material will be occupied by pores (or voids). The conductivity of porous materials decreases with increasing porosity. Hence, low porosity is desirable to maximize the conductivity. However, we know that, fission gases produced during the irradiation tend to swell, i.e., deform the fuel. In order to accommodate the fission gases and limit the swelling a certain degree of porosity is required (usually about 5%). The porosity is defined as:

$$\alpha = \frac{V_p}{V} = \frac{V - V_s}{V} \tag{7.103}$$

where V is the total volume of the pellet, V_p is the volume of the pores and V_s is the volume of the solid. Based on this definition, the density of the oxide fuel is written as:

$$\rho = \rho_s(1-\alpha) + \rho_g\alpha \tag{7.104}$$

where ρ_s and ρ_g are the specific mass of the solid (fuel material) and the gas respectively. In Eq. 7.104, $\rho_g\alpha << \rho_s(1-\alpha)$ and ρ_s is nothing else but the theoretical density, ρ_{TD}, thus we write:

$$\alpha = 1 - \frac{\rho}{\rho_{TD}} \tag{7.105}$$

The ratio ρ/ρ_{TD} is the relative density. The theoretical density of uranium dioxide is 1097 kg/m^3; the relative density is usually 0.95. The Maxwell-Eucken (1932) formula is usually used to determine the effect of the porosity on the conductivity of oxide fuels:

$$k = \frac{1-\alpha}{1+\beta\alpha}k_{TD} \tag{7.106}$$

where k is the conductivity of the porous fuel, k_{TD} is the conductivity of the at theoretical density and β is the pore shape factor ($\beta = 0.5$ for fuel of relative density 0.9 and above; $\beta = 0.7$ for fuels of lower relative density).

Fig. 7.8 illustrates data obtained on the thermal conductivity of unirradiated uranium dioxide as a function of temperature. Data on the conductivity obtained from different sources were corrected to 95% theoretical density using the following relationship:

$$k_{95\%} = k_m\frac{0.95}{1-\alpha} \tag{7.107}$$

where k_m is the measured conductivity. Despite this correction, experimental data show a substantial dispersion. Belle et al. (1967) showed that this scatter was substantially reduced by using Eq. 7.106. On the other hand, Godfrey et al. (1964) and May et al. (1962) noted that the conductivity of uranium dioxide increased as the oxygen-uranium ratio (O/U) is reduced. This stoichiometric effect can account some of the data scatter observed in Fig. 7.8. Numerous

correlations are available for the thermal conductivity of uranium dioxide. Only few of these correlations account for fuel burnup. As reported by Fenech (1981), based on the data appearing in Fig. 7.8, Lyon proposed for an uranium dioxide of 95% of theoretical density the following

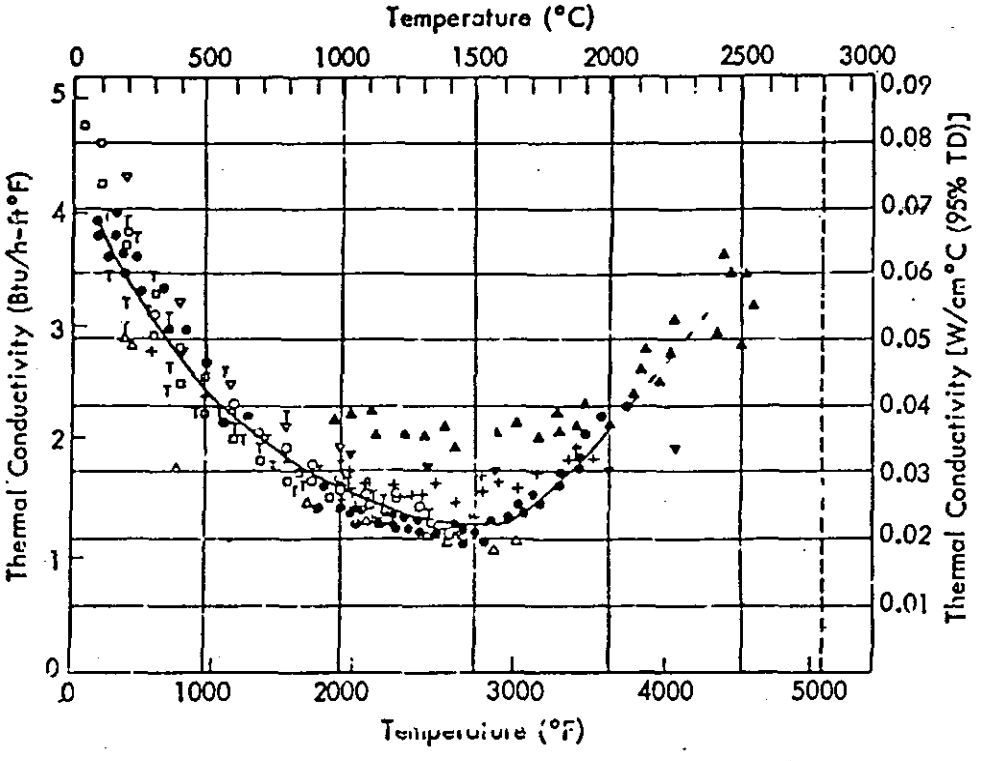

Thermal conductivity of unirradiated UO_2.
Notation ○ Godfrey et al., Ref. 27, 1964.
□ Dayton & Tipton, Battelle Memorial Institute Report BMI-1448, 1960.
▽ Kingery et al., *J. Am. Ceram. Soc.*, 37, 107, 1954.
⊤ Howard & Galvin, UKAEA IG Report 51, 1960.
⊢ Reiswig, *J. Am. Ceram. Soc.*, 44, 48, 1961.
● Nishijima, Ref. 31, 1965.
+ Bush et al., *Trans. Am. Nucl. Soc.*, 7, 392, 1964.
▼ Feith, Ref. 32, 1963.
▲ Feith unpublished data.

Figure 7.8 The thermal conductivity of unirradiated uranium dioxide

correlation:

$$k_{95\%} = \frac{38.24}{402.4+t} + 6.125x10^{-13}(t+273)^3 \quad W/cm\,°C \tag{7.108}$$

where t is the temperature in °C. Since the above correlation is established for a density ratio of 0.95, its application to other density ratios requires the following correction which can be easily obtained from equation from Eq. 7.106:

$$\frac{k}{k_{95\%}} = \frac{1.025}{0.95}\frac{1-\alpha}{1-\alpha\beta} \tag{7.109}$$

As we already pointed out, besides the temperature and the density, the conductivity of the uranium dioxide is also affected by the burnup. A survey by Belle et al. (1967) to take into account the burnup effect as well as the density effect yielded the following correlation:

$$k = \frac{(1-\alpha)}{(1+\beta\alpha)}\left(0.067 + 1.086x10^{-4}T + \frac{3.6}{T} + \frac{28.8}{T^2} + 11.13\frac{F}{T}\right)^{-1} \quad W/m\,°C \tag{7.110}$$

where:

$T = 1.8t + 491.7$; t is the temperature in °C,

F : burnup (fission/cm^3)x10^{-20} .

Once the dependence of uranium dioxide on temperature is known, Eq. 7.90 or 7.91 can be easily integrated to obtain an equation whose solution yields the temperature profile in the fuel element.

It is very difficult to conduct experiments to determine the conductivity of uranium dioxide in the reactor. The insertion of a number of thermocouples at different radial positions is not an easy task and the measurements are subject to a high degree of uncertainty because of the low thermal conductivity and very high temperature gradients that exist in the fuel. Instead it is more convenient to have one measurement in the center of the fuel pellet where the temperature gradient is low. The temperature at the surface of the fuel is deduced from the cladding temperature either by measuring this temperature or calculating from the coolant temperature and local heat generation rate. The measurement is, therefore, the integral of conductivity rather than conductivity. The integral of conductivity is given by Eq. 7.93. This integral is independent of precise knowledge of the conductivity or fuel temperature profile. Besides the fuel surface temperature, the linear heat flux should also be known. Special thermocouples have been used to measure the center temperatures up to 2200 °C; however, the number of high temperature measurements are rather limited. An other way, which is very often used, is based on the indirect determination of the fuel center temperature by tying this temperature to the melting point or to the observable change in the uranium dioxide structure such as grain pattern modifications. About 1500 °C, the uranium dioxide recrystalizes and as already discussed, the new grains are equiaxed. About 1800 °C columnar grains are formed. The melting of uranium dioxide occurs at 2885 °C. Based on the above information, the conductivity integral has been determined and reported by Lyons et al. (1966,1972) and Ogawa et al. (1968). Lyon et al. (1966) reported that the average value of the integral of

conductivity from 0 °C to melting point for sintered uranium pellet of 95% theoretical density is 93.5 w/cm, i.e.,

$$\int_0^{2865} k\,dt = 93.5 \quad W/cm. \tag{7.111}$$

Fig. 7.9 represents the temperature dependence of the conductivity integral. Using this information and the following equation:

$$\int_0^{t_o} k\,dt - \int_0^{t_f} k\,dt = \frac{q'}{4\pi} \tag{7.112}$$

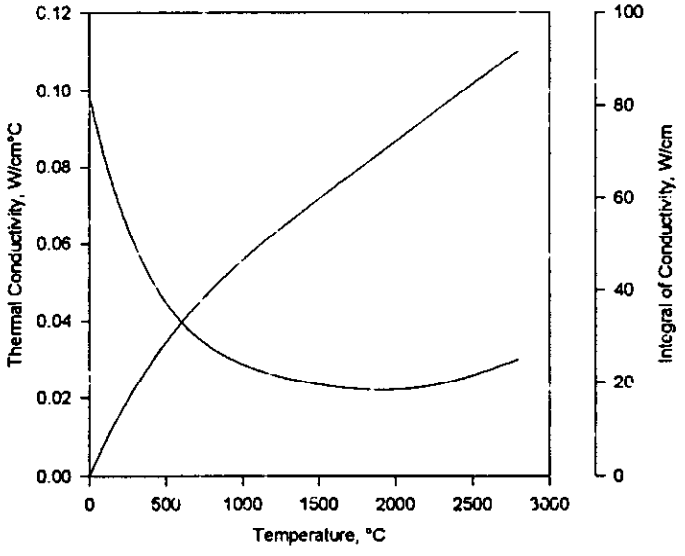

Figure 7.9 Conductivity integral for uranium dioxide pellets with 95% theoretical density, Lyon (1966)

which results from the combination of Eqs. 7.93 and 7.94, the centerline temperature can be determined as follows:

1. using Fig. 7.9 and the surface temperature of the fuel pellet determine the integral:

$$\int_0^{t_f} k\,dt,$$

2. since q' is known, determine using Eq. 7.112 the integral:

$$\int_0^{t_o} k\,dt,$$

3. using again Fig. 7.9 determine the centerline temperature of the fuel pellet.

1.2.4.5 Temperature Distribution in a Fuel Rod with Neutron Flux Depression

In practice, in a fuel rod the heat generation rate is reduced when progressed toward its center. This is due to the fact that the thermalization of the fast neutrons takes place in the moderator. As the thermal neutrons enter the fuel rod from outside, some are absorbed in the outer part of the fuel, and thus the neutron flux is lower in the center. This called neutron flux depression. The theory of neutron diffusion shows that the thermal neutron flux distribution in the radial direction within a fuel rod in a uniform lattice is given by:

$$\phi = \phi_o I_o(\kappa r) \tag{7.113}$$

where:

ϕ_o : value of the thermal neutron flux on the center line of the fuel,

I_o : zero order modified Bessel function of the first kind,

κ : the inverse of the thermal diffusion length in the fuel.

Since the heat sources in the fuel, q''', are proportional to the neutron flux, their distribution is given by:

$$q''' = q'''_o I_o(\kappa r). \tag{7.114}$$

Under above conditions, Eq. 7.84 is written as:

$$\frac{1}{r}\frac{d}{dr}\left(kr\frac{dt}{dr}\right) = -q'''_o I_o(\kappa r). \tag{7.115}$$

Integrating this equation once and knowing that:

$$\int_o^r \kappa r I_o(\kappa r)dr = rI_1(\kappa r) \tag{7.116}$$

we obtain:

$$kr\frac{dt}{dr} = -q'''_o\int_o^r rI_o(\kappa r)dr = -\frac{q'''_o}{\kappa}rI_1(\kappa r). \tag{7.117}$$

Integration of Eq. 7.117 for a second time and knowing that:

$$\int \kappa I_1(\kappa r)dr = I_o(\kappa r) \tag{7.118}$$

we obtain for the integral of conductivity the following relationship:

$$\int_{t_f}^{t} kdt = -\frac{q'''_o}{\kappa^2}\int_{r_o}^{r} \kappa I_1(\kappa r)dr = \frac{q'''_o}{\kappa^2}[I_o(\kappa r_o) - I_o(\kappa r)] \tag{7.119}$$

or for the fuel centerline temperature:

$$\int_{t_f}^{t_o} k\,dt = \frac{q_o'''}{\kappa^2}[I_o(\kappa r_o) - 1]. \tag{7.120}$$

Defining an average heat source (power density) over the entire cross-section of the fuel rod as:

$$\bar{q}''' = \frac{\int_0^{r_o} q''' 2\pi r dr}{\int_0^{r_o} 2\pi r dr} = \frac{2}{r_o^2}\int_o^{r_o} q''' r dr \tag{7.121}$$

and taking into consideration Eqs. 7.114 and 7.116 we can write that:

$$\bar{q}''' = \frac{2q_o''' I_1(\kappa r_o)}{\kappa r_o}. \tag{7.122}$$

Substitution of the above equation into Eqs. 7.119 and 7.120 yields:

$$\int_{t_f}^{t} k\,dt = \frac{q'}{4\pi}\frac{2}{\kappa r_o I_1(\kappa r_o)}[I_o(\kappa r_o) - I_o(\kappa r)] \tag{7.123}$$

and

$$\int_{t_f}^{t_o} k\,dt = \frac{q'}{4\pi}\left[\frac{2}{\kappa r_o}\frac{I_o(\kappa r_o) - 1}{I_1(\kappa r_o)}\right] \tag{7.124}$$

where q' is the linear density given by:

$$q' = \pi r_o^2 \overline{q'''}.$$

If we let

$$f = \left[\frac{2}{\kappa r_o}\frac{I_o(\kappa r_o) - 1}{I_1(\kappa r_o)}\right] \tag{7.125}$$

Eq. 7.124 becomes:

$$\int_{t_f}^{t_o} k dt = f\frac{q'}{4\pi}. \tag{7.126}$$

The term f is called "*flux depression factor*" and it is a function of the fuel enrichment and fuel rod diameter. For natural uranium used in CANDU reactors and for low enriched uranium (~2.5%)

used in PWR reactors, the value of f is slightly smaller than 1. For higher enrichments, f-values become increasingly smaller than 1. The meaning of f becomes clearer when we compare Eqs. 7.93 and 7.126. We observe that the power associated with given surface and center temperature is greater for non uniform than for uniform heat generation; the ratio of two heat rating is f. Obviously when f is close to unity error made by assuming constant heat source is relatively moderate. However, this effect should not be ignored since it can mean an increase of several percentage in reactor power output. Table 7.7 gives an idea on f-values for a uranium dioxide pellet of 95% theoretical density and 9.4 mm in diameter.

Table 7.7 f-values for a fuel pellet of 9.4 mm diameter (Robertson, 1959)

Enrichment, %	$\frac{2}{\kappa r_o}\frac{I_o(\kappa r_o)-1}{I_1(\kappa r_o)}$
0	1
5	0.94
10	0.87
15	0.79
20	0.72

1.2.5 Concluding Remarks on the Fuel Channel Temperatures

A plot of the coolant temperature (Eq. 7.44), the outer surface of the cladding (Eq. 7.49), the surface temperature of the fuel (Eq. 7.77) and centerline temperature of the fuel (Eq. 7.99) along the channel is given in Fig. 7.10. From this figure we observe that the coolant temperature increases continuously from the inlet value to the exit value. However, the temperature of the outer surface of the cladding, the surface of the fuel and the temperature of the fuel centerline rise along the channel and reach maximum values in the second half of the channel beyond the mid-plane of the fuel channel. There are two reasons why the maximum temperatures occur there rather than at mid-channel where the power density (or heat sources) or linear power density (or linear heat flux) is the highest. First, the temperature of the coolant continues to increase steadily past the mid-plane. Second, the linear power is a cosine function and decreases very slowly in the vicinity of the channel mid-plane. But the linear power specify the difference between the temperatures of outer surface of cladding and coolant, fuel surface and coolant, and fuel centerline and coolant. Therefore, with increasing coolant temperature, the fuel element temperatures should also increase to ensure the required heat flow. Further along the channel, the linear power begins to drop more rapidly than the increase of coolant temperature and , consequently, the fuel element temperatures start decreasing. It is this combined effect of a rising coolant temperature and a decreasing linear power that gives rise to and determines the position of the maximum temperature. It is also interesting to note as we move away from fuel center the maximum temperatures shift toward the exit of the fuel channel (Fig. 7.10). To understand the reason of this shift, we will combine Eq. 7.100 with Eqs. 7.50, 7.76 and 7.43 and write as:

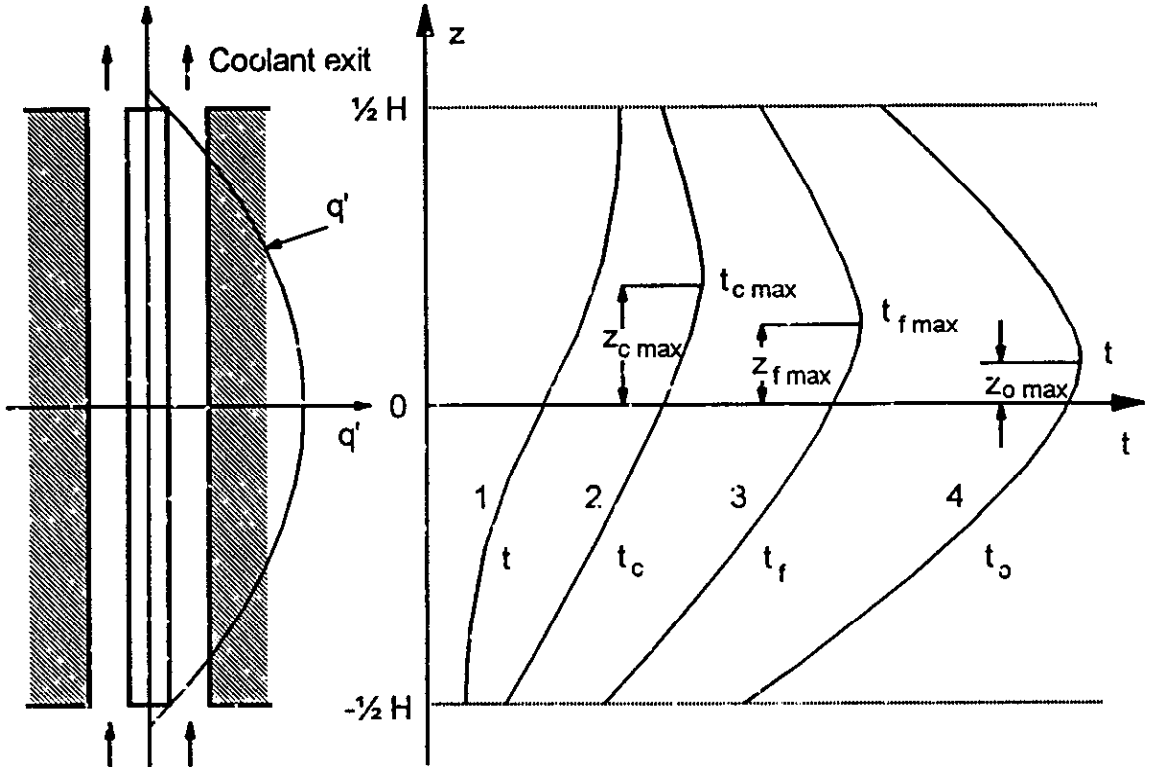

Figure 7.10 Axial temperature distribution in a fuel channel: 1. coolant, 2. outer surface of the cladding, 3. fuel surface and 4. fuel centerline

$$\frac{1}{\gamma''} = \frac{2\beta\,\bar{c}_p\,\dot{m}}{H}\left(\frac{1}{2\pi r_c h_c} + \frac{1}{2\pi k_c}\ln\frac{r_c}{r_o} + \frac{1}{2\pi r_o h_{con}} + \frac{1}{4\pi k_f}\right) \tag{7.127}$$

The first term in the parenthesis is the thermal resistance between the outside surface of the cladding and the coolant, the second term is the resistance of the cladding, the third term id the resistance of the gap region and the forth term is the resistance of the fuel. The leading term, $2\beta\,\bar{c}_p\,\dot{m}\,/\,$, is constant for a given geometry of a channel and operating conditions. Consequently $1/\gamma''$ is proportional to the thermal resistance between the fuel centerline and coolant. As we move away from the fuel centerline, the thermal resistance decreases, therefore:

$$\frac{1}{\gamma} < \frac{1}{\gamma'} < \frac{1}{\gamma''}$$

or

$$\gamma > \gamma' > \gamma''. \tag{7.128}$$

Since the location of the maximum temperature is given by an equation of the following type:

$$z_{max} = a \arctan \tag{7.129}$$

where $b = (\gamma \text{ or } \gamma', \text{ or } \gamma'')$, z_{max} increases as b increases and the maximum temperature shifts further downstream of the mid-plane of the channel. In summary, the location of the maximum temperature is related to the thermal resistance and it shifts further downstream of the channel mid-plane as this resistance decreases. Based on the above discussion, we also argue that increasing the convective heat transfer coefficient, h_c, or decreasing the coolant mass flow rate shifts the point of maximum cladding temperature further away from the fuel channel mid-plane. z_{max} is independent of the power density.

Before closing the discussion, we should emphasize the following points:

1. The knowledge of the cladding and the fuel centerline temperatures is important since together with critical heat flux, discussed in Chapter xx, they imposes limitations on the maximum allowable heat generation in the fuel element.

2. In general, the axial power density profile in a fuel channel is not in the form given by Eq. 7.24 due to fuel and moderator density variations, to the insertion of the control rods and in the CANDU reactors due to the loading and unloading of the fuel bundles.

3. Contrarily to the assumption we have made, the physical properties of the coolant are not constant. The viscosity depends strongly on the temperature. The dependence on the temperature is also true for specific mass, specific heat and conductivity but at a lesser degree. The heat transfer coefficient is usually given by a correlation in the following form:

$$h_c = C\frac{k}{D}\left(\frac{GD}{\mu}\right)^m\left(\frac{c_p\mu}{k}\right)^n, \tag{7.130}$$

is affected by the changes in the physical properties. However, by examining this correlation, we can infer that any changes in physical properties (namely viscosity) will not reflect entirely on the heat transfer coefficient because of the exponents m and n which are less than 1. In general, it is found that if the physical properties are based on the arithmetic mean of the inlet and exit coolant temperature some error on the heat transfer coefficient should be expected (typically 5 to 10%). For a greater accuracy a numerical integration of the conservation equations should be performed along the fuel channel in order to make necessary adjustments to the physical properties as the temperature changes. This observation is particularly true for liquid coolants. For gas coolants, the errors are less severe and can be expected around 3%. When numerical integration is performed, the calculations are refined by using the temperature from the first iteration to define the properties for the second iteration.

1.3 Pressure Drop in Fuel Channels and Pumping Power

In this section we will discuss the pressure drop through the channel, the pumping power required to circulate the coolant and net mechanical power of a fuel channel.

1.3.1 Pressure Drop Through the Fuel Channel

As the coolant flows through the fuel channels in a reactor core, it suffers pressure drop due to the friction between the coolant and walls, to the acceleration as the specific mass of the coolant decreases with increasing temperature, and due to the gravity, if applicable. Acceleration pressure drop is usually small in a liquid cooled reactor but may be significant in a gas cooled reactor or in a reactor where phase change (boiling) takes place.

The total pressure drop gradient in a fuel channel (pressure drop over a unit length is given by:

$$-\frac{dp}{dz}=\left(\frac{dp}{dz}\right)_f+\left(\frac{dp}{dz}\right)_a+\left(\frac{dp}{dz}\right)_g=\frac{4\tau_w}{D}+G^2\frac{d}{dz}v+\rho g \qquad (7.131)$$

where:

p	:	pressure, N/m^2,
τ_w	:	wall shear stress, N/m^2,
D	:	diameter or hydraulic diameter of the channel, m,
G	:	mass flux of the coolant, kg/m^2s,
v	:	specific volume of the coolant, m^3/kg,
ρ	:	specific mass of the coolant, kg/m^3,
g	:	acceleration of the gravity, m/s^2.

The first term on the right hand side of Eq. 7.131 is the pressure drop due to frictional effects discussed in Chapter xx, the second term is the acceleration pressure drop and the third term is the gravitational or elevation pressure drop. From Chapter xx, the frictional pressure drop gradient can be written as:

$$\left(\frac{dp}{dz}\right)_f=\frac{4\tau_w}{D}=\frac{1}{2}f\frac{G^2}{\rho}\frac{1}{D} \qquad (7.132)$$

where f is the friction factor; in the same chapter several correlations were proposed to estimate the value of this factor.

The total pressure drop along the channel, is obtained by integrating Eq. 7.131 over the channel length:

$$\Delta p_T=-\int_{-\frac{1}{2}H}^{\frac{1}{2}H}dp=\int_{-\frac{1}{2}H}^{\frac{1}{2}H}\frac{4\tau_w}{D}dz+\int_{-\frac{1}{2}H}^{\frac{1}{2}H}G^2d(v)+\int_{-\frac{1}{2}H}^{\frac{1}{2}H}\rho g dz. \qquad (7.133)$$

As already pointed out, if the coolant is a liquid and there is no boiling in the fuel channel, the acceleration pressure drop is small compared to frictional pressure thus, it can be neglected. For horizontal fuel channels, seen in CANDU reactors, the gravitational pressure drop is also zero. This pressure drop, even in vertical channels, is usually small compared to frictional pressure drop. Under these conditions, the total pressure drop will consists of only frictional pressure drop and Eq. 7.133 after combining with Eq. 7.132 becomes:

$$\Delta p_T \cong \frac{1}{2} f \frac{G^2}{\rho} \frac{H}{D} \tag{7.134}$$

where H is the fuel channel length. During the integration of Eq. 7.133 it is assumed that the physical properties such as the viscosity and specific mass are constant and, are evaluated at the average channel temperature. Otherwise, Eq. 7.133 can only be integrated by numerical methods.

For gases, neglecting the gravity pressure drop, Eq. 7.133 after combining it with Eq. 7.132 is written as:

$$\Delta p_T = -\int_{-\frac{1}{2}H}^{\frac{1}{2}H} dp = \frac{1}{2} \frac{G^2}{D} \int_{-\frac{1}{2}H}^{\frac{1}{2}H} \frac{f}{\rho} dz + G^2 \int_{-\frac{1}{2}H}^{\frac{1}{2}H} \frac{d}{dz}\left(\frac{1}{\rho}\right) dz. \tag{7.135}$$

The friction factor, f, is usually proportional to $Re^{-0.2}$. The viscosity is the only physical parameter which can influence the value of the Reynolds number along the fuel channel with uniform flow cross-section. In a gas, the viscosity changes rather slowly with temperature, hence the change in f along the channel will be even smaller. Therefore, a value of f determined using the average temperature of the coolant would be appropriate. The specific volume of a gas can be written as:

$$v = v(p, T) \tag{7.136}$$

where T is the absolute temperature. The total derivative of the above equation is:

$$dv = \left(\frac{\partial v}{\partial p}\right)_T dp + \left(\frac{\partial v}{\partial T}\right)_p dT. \tag{7.137}$$

In reactor application, the changes in gas density mainly occurs as a result of temperature changes rather than pressure changes. This arises from the fact that the economic limit of the pumping power is reached when the pressure drop is only a few percent of the absolute pressure, while temperature changes through the reactor may be sufficient to halve the density of the coolant. If we assume that the pressure is constant and equal to

$$\bar{p} = \frac{p_i + p_e}{2} \tag{7.138}$$

Eq. 7.137 becomes:

$$dv \cong \frac{\partial v}{\partial T} dT \tag{7.139}$$

and this average pressure is used to determine the specific volume of the gas. Using Eq. 7.139 and the law of perfect gases:

$$pv = RT \tag{7.140}$$

where R is the perfect gases constant, the acceleration term appearing in Eq 7.135 is written as:

$$G^2\int_{-\frac{1}{2}H}^{\frac{1}{2}H} d\left(\frac{1}{\rho}\right) = G^2\int_{T_1}^{T_2}\frac{R}{\bar{p}}dT = G^2\frac{R}{\bar{p}}(T_e - T_i). \tag{7.141}$$

The above equation can also be written as:

$$G^2\int_{-\frac{1}{2}H}^{\frac{1}{2}H} d\left(\frac{1}{\rho}\right) = \frac{G^2}{\bar{\rho}}\frac{(T_e - T_i)}{\bar{T}} \tag{7.142}$$

where $\bar{\rho} = R\bar{T}/\bar{p}$ and $\bar{T} = (T_i + T_e)/2$; T_i and T_e are inlet and outlet temperatures, respectively. Using Eq. 7.142 and knowing that f can be taken as constant and $\rho = \bar{\rho}$, the pressure drop equation (Eq. 7.135) is written as:

$$\Delta p_T = p_i - p_e = \frac{1}{2}f\frac{G^2}{\bar{\rho}}\frac{H}{D} + \frac{G^2}{\bar{\rho}}\frac{(T_e - T_i)}{\bar{T}}. \tag{7.143}$$

A rather more accurate solution requires to take into account the effect of pressure changes on the specific volume of the gas. Neglecting as usual gravity pressure drop, for a differential length dz, the total pressure drop according Eq. 7.131 is given by:

$$-dp = \frac{1}{\rho}G^2\left(\frac{1}{2}\frac{f}{D}dz + \frac{dv}{v}\right). \tag{7.144}$$

It can be shown that:

$$\frac{dv}{v} = \frac{dT}{T} - \frac{dp}{p}; \tag{7.145}$$

substituting this equation into Eq. 7.144, we obtain:

$$-dp = \frac{G^2}{\rho}\left(\frac{1}{2}\frac{f}{D}dz + \frac{dT}{T} - \frac{dp}{p}\right). \tag{7.146}$$

The integration of this equation can only be carried out numerically. In most of the gas cooled reactors, it will be found that the second term containing the temperature effect term accounts for between 10 and 15% of the total pressure drop whereas the term containing the pressure, the third term, accounts for 1 to 2% of the total pressure. Therefore, in preliminary design calculations, the third term can be ignored and this justifies the approach we have taken at the first place.

The pressure drop calculations we have presented are limited only to the fuel channel. Similar calculations should also be carried out for the hydraulic circuits exterior to the reactor.

1.3.2 Power Required to Circulate the Coolant - Pumping Power

The drop in pressure of the coolant as it flows through the fuel channels (also through the headers, steam generators and piping) must be balanced by the pressure rise across the pump used to circulate the coolant. In producing a given pressure rise in the pump, mechanical energy is added to the coolant; subsequently this mechanical energy is transformed into thermal energy and together with the thermal energy released from the fuel is used by the steam cycle associated to the reactor to generate mechanical (i.e., electrical) energy with an efficiency of about 30%. The use of electrical energy in driving the pumps, and subsequent reconversion to electrical energy with the above efficiency, will reduce the overall thermal efficiency of the plant. Moreover, when the power input to the pumps increases, the size and the cost also increases.

In gas cooled reactors, the optimum value of the pumping power is generally between 2 and 5 % of the heat output of the reactor which corresponds about 6 to 15% of the electrical output. In liquid cooled reactors, because of the higher coolant density, the pumping power represents 3 to 4 % of the electrical output.

The Pumping power is calculated by using the energy conservation law for an open system (flowing system) which has the following form:

$$Q + W = \dot{m}\,(h_2 - h_1) + \frac{1}{2}\,\dot{m}\left(w_2^2 - w_1^2\right) + \dot{m}\,g(z_2 - z_1) \qquad (7.147)$$

where

Q	:	the rate of heat input to the fluid, kJ/s,
W	:	the rate of work input to the fluid, kJ/s,
$\dot{m}$	:	mass flow rate, kg/s
h	:	enthalpy, kJ/kg
w	:	velocity, m/s
g	:	acceleration of the gravity, m/s^2
z	:	elevation, m
1,2	:	inlet and exit conditions, respectively

In the present application, we can assume that the changes in kinetic energy (second term on the r h.s.) and potential energy (third term on the r.h.s.) may be neglected. In a pump where no heat is exchanged with working fluid, Q will be equal to zero, therefore, Eq. 7.147 becomes:

$$W = \dot{m}\,(h_2 - h_1). \qquad (7.148)$$

Remembering the thermodynamic relationship (Sontag and Van Wylen, 1991):

$$dh = Tds + vdp$$

and assuming that there are no internal losses due to friction of the fluid as it goes through the pump (i.e., isentropic process), the enthalpy change is given by:

$$dh \cong v\,dp. \tag{7.149}$$

For reactor coolants, the specific volume is roughly constant, either because the coolant is a liquid and virtually incompressible, or in the case of gases because the absolute pressure of the gas, at, for example, 40 bars, is much higher than the change of pressure across the pump, which is about 3 bars. Therefore, the integration of Eq. &.149 yields:

$$\int_{h_1}^{h_2} dh = \int_{p_1}^{p_2} v\,dp \tag{7.150}$$

or

$$h_2 - h_1 = v(p_2 - p_1) = v\Delta p. \tag{7.151}$$

Substituting this equation into Eq. 7.148, we obtain the pumping power as:

$$W = \dot{m}\ v\Delta p\,. \tag{7.152}$$

Although Eq. 7.152 gives the power necessary to circulate the coolant, the power required to drive the pumps si greater than this by a factor $1/\eta_p$ where η_p is the combined mechanical and electrical efficiency of the pump motors. The pumping power is, therefore, given by:

$$\mathbf{P}_p = \frac{W}{\eta_p} = \frac{\dot{m}\ v\Delta p}{\eta_p}\,. \tag{7.153}$$

By examining the above equation, we conclude that in order to minimize the pumping power, the specific volume should be as small as possible. Consequently, the circulating pumps should be placed to the coolest point in the circuit, namely at the inlet of the reactor.

As already pointed out Δp represents the pressure drop in the fuel channels, inlet and outlet headers, steam generators and in the piping system. However, during the preliminary design phase, no detailed information is available on the circuit outside of the fuel channel. In such case, the pumping power is estimated based on the fuel channel total pressure drop. The pumping power is than multiplied by a factor "e"(> 1) to account for the pressure drop in the circuits outside the fuel channel and written as follows:

$$\mathbf{P}_{pe} = e\frac{\dot{m}\ v\Delta p_c}{\eta_p}. \tag{7.154}$$

where Δp_{ch} is the total pressure drop in the fuel channel.

1.4 Net Mechanical Power of the Fuel Channel

The heat energy produced in the channel (reactor core) is used to produce electric power. During this conversion the temperature of the coolant decreases from t_e to t_i and heat is extracted from the coolant. The Second Law of Thermodynamics states that it is impossible to convert the extracted heat entirely and continuously in the work. Therefore power engineers endeavor to convert as much as possible this heat energy into mechanical energy. The thermodynamic efficiency of a power cycle is the ratio of the work output to the heat received.

The basic thermodynamic cycle is the Carnot cycle. In this cycle, all heat is received isothermally at a temperature T_h and all heat is rejected isothermally at a lower temperature T_c. All the processes in the cycle are reversible and its thermal efficiency is given by:

$$\eta_c = 1 - \frac{T_c}{T_h}. \tag{7.155}$$

When the temperature of the coolant leaving the reactor decreases from t to $t - dt$, it releases per unit mass a certain amount of heat energy which is equal to the variation of its enthalpy shown by *dh*. This heat energy can be transformed into work with a maximum efficiency given by:

$$\eta_c = 1 - \frac{T_c}{T}. \tag{7.156}$$

The total heat released by the coolant when its temperature decreases from t_e to t_i (or its enthalpy decreases from h_e to h_i) is given by:

$$\mathbf{P}_c = \int_{h_i}^{h_e} dh = \int_{T_i}^{T_e} \bar{c}_p dT \tag{7.157}$$

where T is the absolute temperature. The maximum work that can be recovered from this heat is:

$$\mathbf{W}_{\max} = \int_{T_i}^{T_e} \left(1 - \frac{T_c}{T}\right) dh = \int_{T_i}^{T_e} \left(1 - \frac{T_c}{T}\right) c_p dT. \tag{7.158}$$

The efficiency of this *ideal conversion* is given by:

$$\eta_c = \frac{\mathbf{W}_{\max}}{\mathbf{P}_c} = \frac{\int_{T_i}^{T_e} \left(1 - \frac{T_c}{T}\right) \bar{c}_p dT}{\int_{T_i}^{T_e} \bar{c}_p dT} = 1 - \frac{T_c}{T_{av}} \tag{7.159}$$

where T_{av} is the logarithmic mean temperature of the coolant and defined as:

$$T_{av} = \frac{T_e - T_i}{\ln \frac{T_e}{T_i}}. \tag{7.160}$$

If the ratio of T_e/T_i is close to 1, using the approximation:

$$\ln x \cong 2\frac{x-1}{x+1} \tag{7.161}$$

where x is equal to T_e/T_i, Eq. 7.160 can be written as:

$$T_{av} = T_m = \frac{T_e + T_i}{2} \tag{7.162}$$

and the efficiency of the ideal conversion is:

$$\eta_c = 1 - \frac{T_c}{T_m}. \tag{7.163}$$

In CANDU reactors, typical inlet and exit temperatures of the coolant are 267 °C and 312 °C, respectively. According to Eqs. 7.160 and 7.162 the logarithmic and arithmetic mean temperature of the coolant are 289.2 °C and 289.5 °C, respectively. Therefore, the approximation given by Eq. 7.161 is a reasonable one.

From the above discussion, we conclude that if the energy conversion system were ideal one, the heat energy converted into mechanical energy would be:

$$\mathbf{W}_{\max} = \eta_c \mathbf{P}_c. \tag{7.164}$$

However, the real energy conversion systems are far being perfect and have several irreversibilities such as friction, heat transfer with finite temperature difference, etc. and their efficiency is less than then the efficiency of the ideal systems. Introducing a factor "η_r" < 1to take into account the irreversibilities, the *recoverable mechanical energy* is given by:

$$\mathbf{W} = \eta_r \eta_c \mathbf{P}_c = \eta \mathbf{P}_c \tag{7.165}$$

η is interpreted as the combined thermal efficiency of the steam cycle and the efficiency of the turbo-generators. The efficiency of nuclear power plants is about 30%. In Eq. 7.165, $\mathbf{P}_c$ shows the thermal output of the fuel channel. In calculating the total thermal output of the channel, $\mathbf{P}_T$, the power to circulate the coolant, given by $\eta_p \mathbf{P}_p$, should be added to the thermal power of the channel:

$$\mathbf{P}_T = \mathbf{P}_c + \eta_p \mathbf{P}_p. \tag{7.166}$$

The gross electrical power is then given by:

$$\eta(\mathbf{P}_c + \eta_p \mathbf{P}_p)$$

and the net electrical power with:

$$\mathbf{W}_{net} = \eta(\mathbf{P}_c + \eta_p \mathbf{P}_p) - \mathbf{P}_p = \eta \mathbf{P}_c - (1 - \eta\eta_p)\mathbf{P}_p. \tag{7.167}$$

The overall efficiency of the fuel is then:

$$\eta_{net} = \frac{\mathbf{W}_{net}}{\mathbf{P}_c} = \eta - (1 - \eta\eta_p)\frac{\mathbf{P}_p}{\mathbf{P}_c}. \tag{7.168}$$

The efficiency of the pumps varies between 65% and 95%. In PWR and CANDU reactors this efficiency is between 90% and 92%.

1.4.1 Optimum Operating Point of a Channel

To discuss the optimum operating point of a fuel channel, in Eq. 7.166 we will assume that $\eta_p \mathbf{P}_p$ is much smaller than $\mathbf{P}_c$,thus it can be neglected. In liquid cooled reactors, $\eta_p \mathbf{P}_p$ is only 1% of the thermal output of the reactor; this justify this assumption and we write:

$$\mathbf{P}_T \cong \mathbf{P}_c. \tag{7.169}$$

Knowing that the mass flux of the coolant in the fuel channel is given by:

$$G = \frac{\dot{m}}{A} = \frac{\mathbf{P}_c}{\bar{c}_p(t_e - t_i)A} \tag{7.170}$$

the pressure drop of the channel given by Eq. 7.134 can be written as:

$$\Delta p_T = \frac{1}{2} f \frac{\mathbf{P}_c^2}{(t_e - t_i)^2} \frac{1}{\rho \bar{c}_p^2} \frac{H}{DA^2}. \tag{7.171}$$

To progress further, we will assume that the friction coefficient is given by:

$$f = 0.184 Re^{-0.2} \tag{7.172}$$

where Re is the Reynolds number and given by:

$$Re = \frac{GD}{\mu}. \tag{7.173}$$

Substituting Eqs. 7.172 and 7.173 into Eq. 7.171, we obtain for the pressure drop the following equation:

$$\Delta p_T = 0.092 \frac{\mathbf{P}_c^{1.8}}{(t_e - t_i)^{1.8}} \frac{\mu^{0.2}}{\rho \bar{c}_p^{1.8}} \frac{H}{D^{1.2} A^{1.8}} \tag{7.174}$$

From this equation, we conclude that for a given temperature rise in the fuel channel, the pressure drop increases as 1.8 power of the heat output of the fuel channel.

For the pumping power of the channel we can easily write:

$$\mathbf{P}_p = \frac{\dot{m}}{\rho} \frac{1}{\eta_p} \Delta p_T = 0.092 \frac{1}{\eta_p} \frac{\mathbf{P}_c^{2.8}}{(t_e - t_i)^{2.8}} \frac{\mu^{0.2}}{\rho^2 \bar{c}_p^{2.8}} \frac{H}{A^{1.8} D^{1.2}}. \tag{7.175}$$

We observe that the pumping power increases with 2.8 power of the heat output of the channel. The net electrical output of the channel is given by:

$$\mathbf{W}_{net} = \eta \mathbf{P}_c - 0.092 \frac{1}{\eta_p} \frac{\mathbf{P}_c^{2.8}}{(t_e - t_i)^{2.8}} \frac{\mu^{0.2}}{\rho \bar{c}_p^{2.8}} \frac{H}{A^{1.8} D^{1.2}}. \tag{7.176}$$

This equation can also be written as:

$$\mathbf{W}_{net} = \eta \mathbf{P}_c - a\mathbf{P}_c^{2.8}. \tag{7.177}$$

If we keep the average coolant temperature constant (by increasing the coolant flow rate with channel power), "a" in Eq. 7.177 remains constant. The maximum of the above function is easily determined by deriving it with respect to $\mathbf{P}_c$ and equating it to zero:

$$\eta - 2.8a\mathbf{P}_c^{1.8} = 0 \tag{7.178}$$

The value of $\mathbf{P}_c$ corresponding to the maximum net operating power is then given by:

$$\mathbf{P}_c^{1.8} = \frac{\eta}{2.8a}$$

or

$$\mathbf{P}_c = \frac{\eta^{0.56}}{1.77a^{0.56}} \tag{7.179}$$

Beyond the above value of the channel power, the net electric power output of the channel will start falling because of the high pumping power required to circulate the coolant. The value of the maximum electrical power output of the channel can be easily determined by substituting Eq. 7.179 into Eq. 7.177.

1.5 The Choice of Coolant for Reactors

The coolant for a nuclear reactor may be either a gas such as carbon dioxide or helium, or liquid such as light or heavy water, or liquid metal such as sodium or eutectic sodium-potasium alloy. In selecting the coolant, the following considerations should be taken into account.

1. Economics: low cost, availability, low pumping power, high heat transfer coefficient.
2. Physics: low fusion point, high boiling temperature, good compatibility with fuel, cladding, pump, valves, piping, etc., good thermal stability.
3. Neutronics: low neutron capture cross-section, moderating power compatible with the type of the reactor (thermal or fast), low induced radioactivity, short lived radioactivity, good stability under irradiation.

Helium and carbon dioxide are the most suitable gases. The cost of helium has prevented its use in large power reactors in which the leakage of the coolant gas may be significant; future high temperature gas cooled reactors may use helium. Water and heavy water are suitable in most respects for thermal reactors in which they can fulfill dual moderating and cooling roles. However, they have the great disadvantage that the high coolant temperatures require high system pressures, i.e., thick pressure vessels or tubes. The capture cross-section of light water is high and enriched uranium fuel is required to achieve the criticality of the reactor. On the other hand, heavy water has

very low capture cross-section but is very expensive. Both light and heavy water require stainless steel or zircalloy cladding.

Sodium and the eutectic sodium-potasium alloy are the most common liquid metal coolants. They have high saturation temperature at atmospheric pressure so that a pressurized coolant system is unnecessary. However, $^{23}Na(n,\gamma)^{24}Na$ reaction produces a radiation hazard. The violent chemical reactions between sodium and air or water make it essential to eliminate the possibility of coolant leakage. The capture cross-section of sodium is rather high for its use as coolant in thermal reactors, and this point together with its non-moderating characteristics make it more suitable coolant for fast reactors.

A good comparison of the performance of different coolants can be undertaken by examining the ratio of the pumping power (given by Eq. 7.175) and channel heat power (given by Eq. 7.43); this ratio has the following form:

$$\frac{\mathbf{P}_p}{\mathbf{P}_c} = \left[0.092\frac{1}{\eta_p}\frac{\mathbf{P}_c^{1.8}}{(t_e - t_i)^{2.8}}\right]\left[\frac{\mu^{0.2}}{\rho^2 \bar{c}_p^{2.8}}\right]\left[\frac{H}{D^{1.2}A^{1.8}}\right]. \tag{7.180}$$

In the above equation the firs bracket is related to the operating point of the channel, the second to the physical properties of the coolant and the third to the geometry of the channel. From coolant point of view, the second bracket should be as small as possible to ensure a minimum $\mathbf{P}_p/\mathbf{P}_c$ ratio. This is only achieved for light and heavy water.

A better discussion of the coolant effect can be carried out by writing that:

$$\mathbf{P}_c = h_c S \Delta t_f \tag{7.181}$$

where:

h_c	:	heat transfer coefficient between the fuel rod and coolant, kW/m^2 °C,
S	:	heat transfer surface, m^2,
Δt_f	:	average temperature difference for the channel between the fuel element surface and coolant, °C.

We will assume that the heat transfer coefficient is given by Dittius-Boelter correlation (Chapter xx) with n=0.4:

$$h_c = 0.023\frac{k}{D}\left(\frac{GD}{\mu}\right)^{0.8}\left(\frac{\bar{c}_p\mu}{k}\right)^{0.4}. \tag{7.182}$$

Dividing Eq. 7.175 by Eq. 7.181 and taking into account Eq. 7.182, we obtain for the $\mathbf{P}_p/\mathbf{P}_c$ ratio the following equation:

$$\frac{\mathbf{P}_p}{\mathbf{P}_c} = 4\left[\frac{1}{DSA}\right]\left[\frac{\mathbf{P}_c^2}{\Delta t^2 \Delta t_f}\right]\left[\frac{1}{\rho^2 \bar{c}_p^2}\left(\frac{k}{\bar{c}_p\mu}\right)^{0.4}\frac{\mu}{k}\right] \tag{7.183}$$

where $\Delta t = (t_e - t_i)$. In the above equation, the physical properties of the coolant appear in the last bracket. In order to achieve minimum $\mathbf{P}_p/\mathbf{P}_c$ ratio this group should be as small as possible. Galliland (1949) compared several coolants from the point of view of physical properties group appearing in Eq. 7.183. Physical properties of the gas coolants were calculated at 0 °C and those of the liquids at 80 °C. The results of this comparison is shown in table 7.7.

Table 7.7 Comparison of the coolants

Gas	$\left[\frac{1}{\rho^2 \bar{c}_p^2}\left(\frac{k}{\bar{c}_p \mu}\right)^{0.4} \frac{\mu}{k}\right]$	$\frac{X}{X_{H_2}}$	Liquids	$\left[\frac{1}{\rho^2 \bar{c}_p^2}\left(\frac{k}{\bar{c}_p \mu}\right)^{0.4} \frac{\mu}{k}\right]$	$\frac{X}{X_{H_2}}$
H_2	662	1.0	H_2O	0.0004425	1.0
He	3,315	5.1	*Na	0.0008770	2.0
H_2O	5,040	7.7	*Hg	0.0033500	7.6
CO_2	6,560	10.1	*Bi	0.0053000	12.0
Air	8,150	12.5	Glycol	0.0091900	20.8
N_2	8,740	13.4	Freon-12	0 0095700	21.6

* A different correlation for heat transfer coefficient has been used.

Among the gas coolants, according this criterion, the hydrogen is the best coolant followed by helium and steam. However, these three gases have several drawbacks to be used as coolant in reactors (explosion for hydrogen, high cost for helium, high pressure and corrosion for steam). Therefore, only carbon dioxide seems to be an acceptable gaseous coolant Air and nitrogen have serious activation problems. Among liquid coolants, water (light and heavy) is, incontestably, the best coolant followed by liquid metals. It should be again emphasized that the above discussion is based only on the physical properties of the coolants and doesn't take into consideration other criteria for the coolant selection as listed above.

REFERENCES

Kenard, F. H., "Kinetic Theory of Gases, " 1st ed., pp. 311-325, McGraw-Hill Book Company, New York, 1938.

?Kampf, H. and Karsten, G.," ," Nucl. Appl. Techno., 9, pp. 288, 1970.

Cetinkale, T. N. and Fishenden, M., "Thermal Conductance of Metal Surfaces in Contact," Proc. General Discussion on Heat Transfer, Institute of Mechanical Engineers, London, 1951.

Ross, A.M. and Stoute, R.L., "Heat Transfer Coefficient Between UO_2 and Zircaloy-2," AECL-1552, 1962.

?INSTN - Cours de génie atomique, Presse Universitaire de France, 1960.

?Tong, L. S., "Heat Transfer in Water Cooled Nuclear Reactors," Nucl. Eng. and Design, 6, pp. 301- , 1967.

?MacDonald, P.E. and Thompson, L.B., "MATPRO-Handbook of Material Properties for Use in Analysis of Light Water Reactor Fuel Rod Behavior," Idaho Nuclear Engineering Laboratory, 1976.

?Godfrey, T.G., Fulkerson, W., Kollie, T.G., Moore, J.P. and McElroy, D.L., "Thermal Conductivity of Uranium Dioxide and Armco Iron by an Improved Radial Flow Technique," ORNL-3556, Oak Ridge National Laboratory, 1964.

May, J.F., Notley, M.J.F., Stoute, R.L. and Robertson, A.L. "Observation on Thermal Conductivity of Uranium Dioxide," AECL-1641, Atomic Energy of Canada limited, 1962.

Belle, J., Berman, R.M., Bourgeois, W.F., Cohen, J. and Daniel, R.C. "Thermal Conductivity of Bulk Oxide Fuels," WAPD-TM-586, Bettis Atomic Power Laboratory, 1967.

?Eucken, A. Forsch. Geb. Ingenieurw., B3, Forschungshaft no: 353, 1932.

Fenech, H. Editor, Heat Transfer and Fluid Flow in Nuclear Systems, Pergamon Press, 1981.

Lyons, M.F., Boyle, R.F., Davies, J.H., Hazel, V.E. and Rowland, T.C. "UO_2 Properties Affecting Performance," Nucl. Eng. and Design, 21, pp. 167-199, 1972.

Lyons, F.M. et al. "UO_2 Powder and Pellet Thermal Conductivity During Irradiation," GEAP-5100-1, 1966.

Ogawa, S.Y., Lees, E.A. and Lyons, M.F., "Power Reactor High Performance UO_2 Program. Fuel Design Summary and Program Status," GEAP-5591, 1968.

Robertson, J.A.L. "$\int k d\theta$ in Fuel Irradiations," AECL-807, 1959.

Sonntag, R.E. and Van Wylen, G.J. "Introduction to Thermodynamics - Classical and Statistical," 3rd. Edition, John Willey & Sons, pp. 197-198, 1991.

Galliland, E.R. "The Science and Engineering of Nuclear Reactors," 1949.

SPELL CHECK